Department of Geodetic Science

BASIC RESEARCH FOR THE EARTH DYNAMICS PROGRAM

Sixth Semiannual Status Report
Research Grant No. NSG 5265
OSURF Project No. 711055

Third Semiannual Status Report
Research Contract NAS5-25888
OSURF Project No. 712407

Period Covered: October 1, 1980 - March 31, 1981

Prepared for

NASA/Goddard Space Flight Center
Greenbelt, Maryland 20771

The Ohio State University
Research Foundation
Columbus, Ohio 43212

April, 1981

PREFACE

These projects are under the supervision of Professor Ivan I. Mueller, Department of Geodetic Science, The Ohio State University. The Science Advisor of RF 711055 is Dr. David E. Smith, Code 921, Geodynamics Branch, and the Technical Officer is Mr. Edmond C. Holweck, Code 902.2, Technology Applications Center. The Technical Officer for RF 712407 is Mr. C. Stephanides, Code 942. The latter three are at NASA/GSFC, Greenbelt, Maryland 20771.

TABLE OF CONTENTS

1. TECHNICAL OBJECTIVES

1. Optimal Utilization of Laser and VLBI Observations for Reference Frames for Geodynamics (Grant NSG 5265)
2. Optimal Utilization of Satellite-Borne Laser Ranging System (Grant NSG 5265)
3. Geodetic Utilization of NAVSTAR Geodetic Positioning System (Grant NSG 5265)
4. Utilization of Range Difference Observations in Geodynamics (Contract NAS 5-25888)

2. ACTIVITIES

2.1 Comparison of Data from Project MERIT Short Campaign

2.11 Prediction of Polar Motion

Based on the analysis of polar motion behavior, we found the possibility of predicting polar motion for a long time interval (1-2 years in advance) with sufficient accuracy. We take the best estimated Chandler period as constant, use six years of data to estimate the amplitudes, phases and ellipticity (only for annual) of Chandler and annual motion. These estimated parameters are then used to predict the next year's (or next two years') polar motion. In making the prediction, we also take the linear trend into consideration.

The data used for prediction are BIH, IPMS, and DMA, with the time interval from 1968 to 1980 (DMA data from 1972 to 1980). We predicted polar motion one yar in advance, compare the predicted polar coordinates with the real observed ones (smoothed); the mean rms of the differences (predicted minus observed) is about 0".02. The differences of the relative polar motion are much smaller. For a time interval of 20-30 days, the rms of relative polar motion differences is about 0".01 (30 cm) through the whole year. Compared with the best available VLBI results (from 1977 to 1980), the rms of predicted - observed is 0".013; and the relative rms (with time interval less than or equal to two months) is 0".008; here the VLBI observed data is unsmoothed.

The predicted polar motion can be used for geodetic purposes. It also seems that the accuracy of polar motion prediction is high enough for any purposes that require the real time polar motion value, including the control of spaceships.

Theoretically, we can say that about 90 percent of polar motion is composed of the stable, predictable Chandler and annual terms.

We also analyzed the error sources in polar motion prediction. In doing so, we found that in DMA data there are systematic differences among the polar coordinates determined by different satellites. Details may be found in "Prediction of Polar Motion" by Y.S. Zhu, Dept. of Geodetic Science, 1981, in press.

2.12 MERIT Short Campaign Data Analysis

The BIH has already analysed the MERIT data using BIH Circular D as a common reference. Since new techniques are expected to obtain better accuracy than now achieved by the BIH, we think that a mutual comparison method may be more rational than using BIH Circular D as a common reference. In analyzing, we use both raw data and smoothed data.

2.121 Using Raw Data

Direct comparison. We compute the standard deviation of the polar coordinate differences of each two Analyzing Centers. The results are as follows:

	$\sigma_{\Delta x}$	$\sigma_{\Delta y}$	mean
DMA - MEDOC	0".040	0".044	0".042
$CNS_{(39)}$ - $CNS_{(10)}$	0.031	0.053	0.042
SAO - $CNS_{(10)}$	0.040	0.036	0.038
CLA(Opt.) - SAO	0.022	0.025	0.024
CLA(Opt.) - DMA	0.022	0.025	0.023
CLA(Opt.) - UTX	0.019	0.026	0.023
DMA - SAO	0.010	0.011	0.011
UTX - SAO	0.014	0.012	0.013
UTX - DMA	0.014	0.010	0.012
SAO - $CNS_{(39)}$	0.009	0.014	0.012
UTX - $CNS_{(39)}$	0.010	0.017	0.014

From the above values we suggest that the standard errors of each Analyzing Center are approximately: 0".01 for MEDOC and for $CNS_{(10)}$, 0".02 for classical (optical), 0".008 - 0".01 for SAO, DMA, UTX and $CNS_{(39)}$.

Relative polar motion comparison. Relative polar motion comparison is used to detect the possible systematic error (other than constant systematic error--the difference of origin). Systematic error will be mostly reduced in relative polar motion, while it remains in direct comparison.

The standard error of relative polar motion along with the standard error obtained in direct comparison are given below.

	Relative			Direct		
	$\sigma_{\Delta x}$	$\sigma_{\Delta y}$	σ_{mean}	$\sigma_{\Delta x}$	$\sigma_{\Delta y}$	σ_{mean}
DMA - MEDOC	0".039	0".039	0".039	0".040	0".044	0".042
SAO - UTX	0.010	0.010	0.010	0.014	0.012	0.013
DMA - UTX	0.014	0.008	0.011	0.014	0.010	0.012
DMA - SAO	0.010	0.009	0.010	0.010	0.011	0.011
Opt. - SAO	0.017	0.022	0.020	0.022	0.025	0.024
Opt. - DMA	0.024	0.022	0.023	0.022	0.025	0.023
Opt. - UTX	0.017	0.024	0.021	0.019	0.026	0.024
SAO - Circular D	0.005	0.004	0.005	0.009	0.009	0.009
UTX - Circular D	0.011	0.010	0.010	0.011	0.013	0.012

Since every σ_{direct} is more or less larger than $\sigma_{relative}$, it means that there are systematic errors among the Analyzing Centers. The detailed properties of the systematic errors (say, the period, amplitude, etc.) could not be obtained because of the short time span of data available.

2.122 Intercomparison After Smoothing

In the initial stage direct comparison gave reasonably good evidence that systematic differences exist between the results of the earth rotation parameters obtained from different techniques. Later a smoothing process (by adjustment) was used by adopting a suitable mathematical model for intercomparison of pole positions obtained from different methods during the MERIT Short Campaign. The mathematical model used is given below.

$$x = k_1 + k_2 \cos A + k_3 \sin A + k_4 \cos c + k_5 \sin c$$
$$y = k_6 - k_2 \sin A + k_3 \cos A - K_4 \sin c + k_5 \cos c$$

where $A = 2PI\ (MJD - 42413)/365$

$c = 2PI\ (MJD - 42413/435$

k_1 to k_6 are coefficients in seconds of arc

The smoothed x, y coordinates of the pole were plotted in each case, and it was seen that curves depicting the motions were of different shapes and were at different locations with respect to the origin (CIO). These plots are Figs 1 to 7.

As a consequence of the smoothing process, the values of coefficients k_1 and k_6 obtained were plotted on a graph with their standard deviations (Fig. 8). k_1 and k_6 correspond to x and y coordinates of the origin of the curve, depicting the pole movements with respect to the CIO. This figure shows that systematic differences exist in the pole origin recovered as a result of these different techniques, which may be due to differences in mathematical models for computations and locations of observing stations, etc. Figs. 1 to 7 also give preliminary evidence that there is a systematic difference existing in the values of annual and Chandler period amplitudes recovered by different techniques.

The data available for the MERIT Short Campaign was not really sufficient to enable us to arrive at any conclusive evidence regarding the systematic differences and their estimation; and the noise level was also quite high. Therefore, we should wait for the intercomparison of data to be made available through the MERIT Main Campaign.

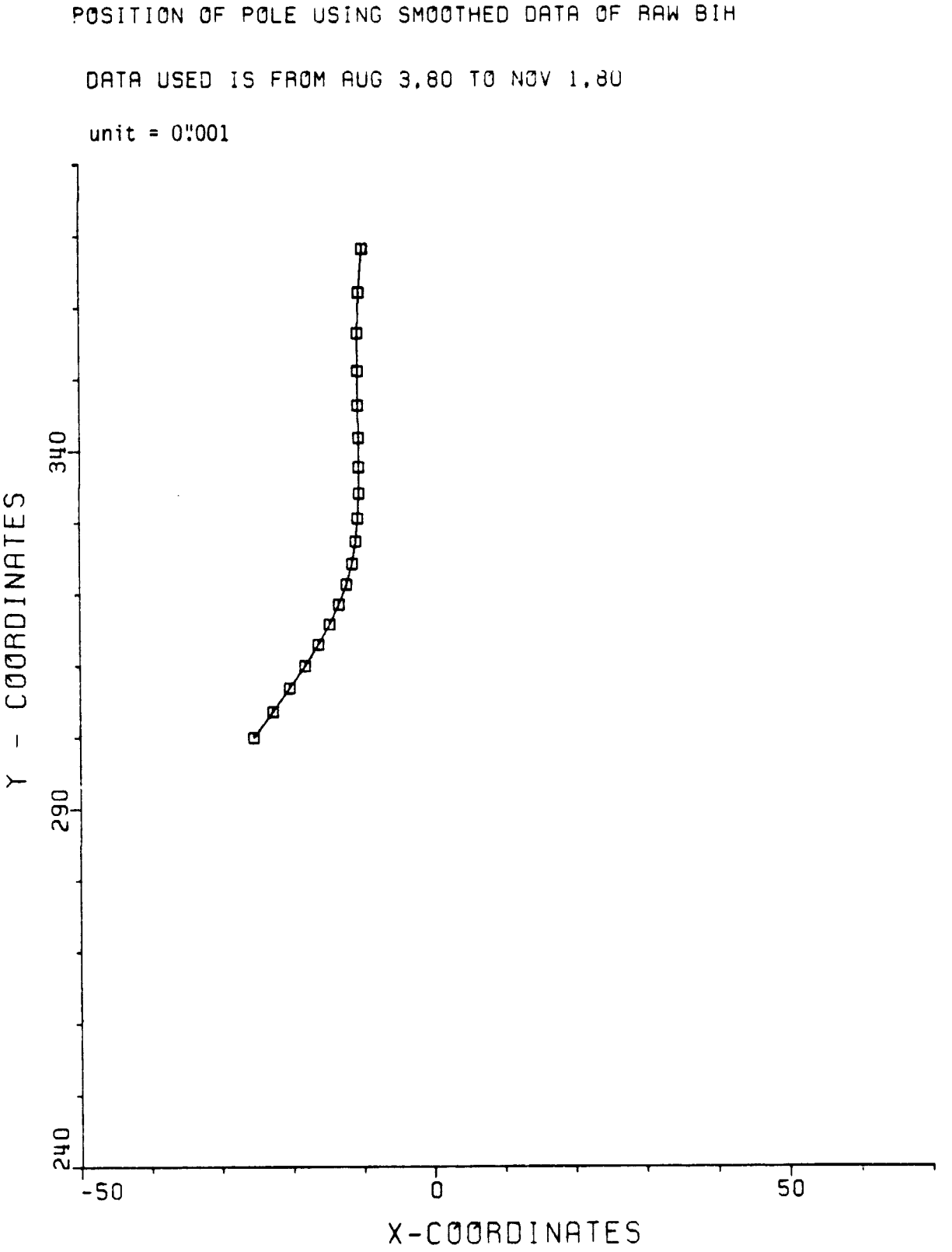
POSITION OF POLE USING SMOOTHED DATA OF RAW BIH
DATA USED IS FROM AUG 3,80 TO NOV 1,80
unit = 0".001
Y - COORDINATES
340
290
240
-50
0
50
X-COORDINATES

Fig. 1

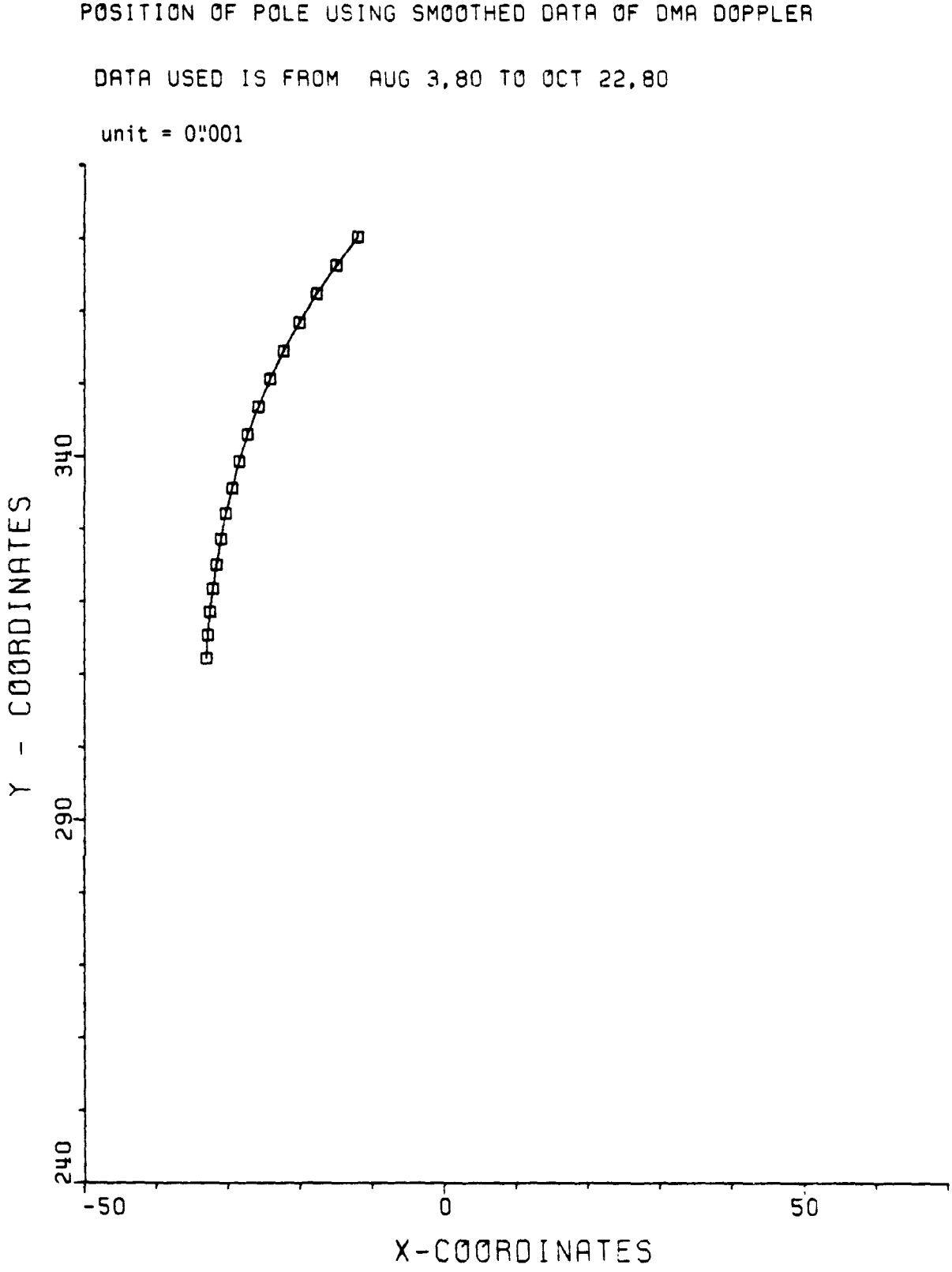
POSITION OF POLE USING SMOOTHED DATA OF DMA DOPPLER
DATA USED IS FROM AUG 3,80 TO OCT 22,80
unit = 0".001
Y - COORDINATES
340
290
240
-50
0
50
X-COORDINATES

Fig. 2

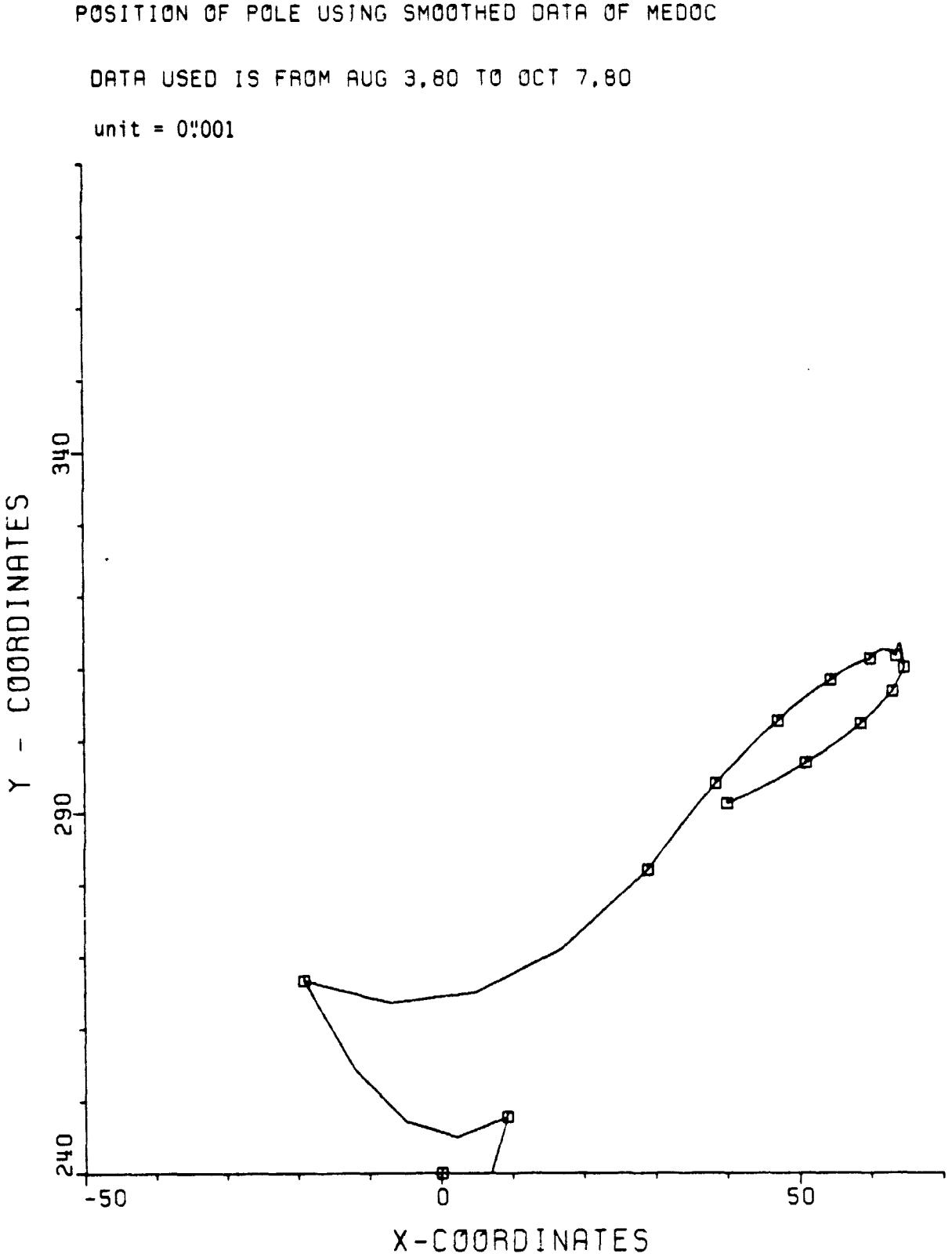
POSITION OF POLE USING SMOOTHED DATA OF MEDOC
DATA USED IS FROM AUG 3,80 TO OCT 7,80
unit = 0".001
Y - COORDINATES
340
290
240
-50
0
50
X-COORDINATES

Fig. 3

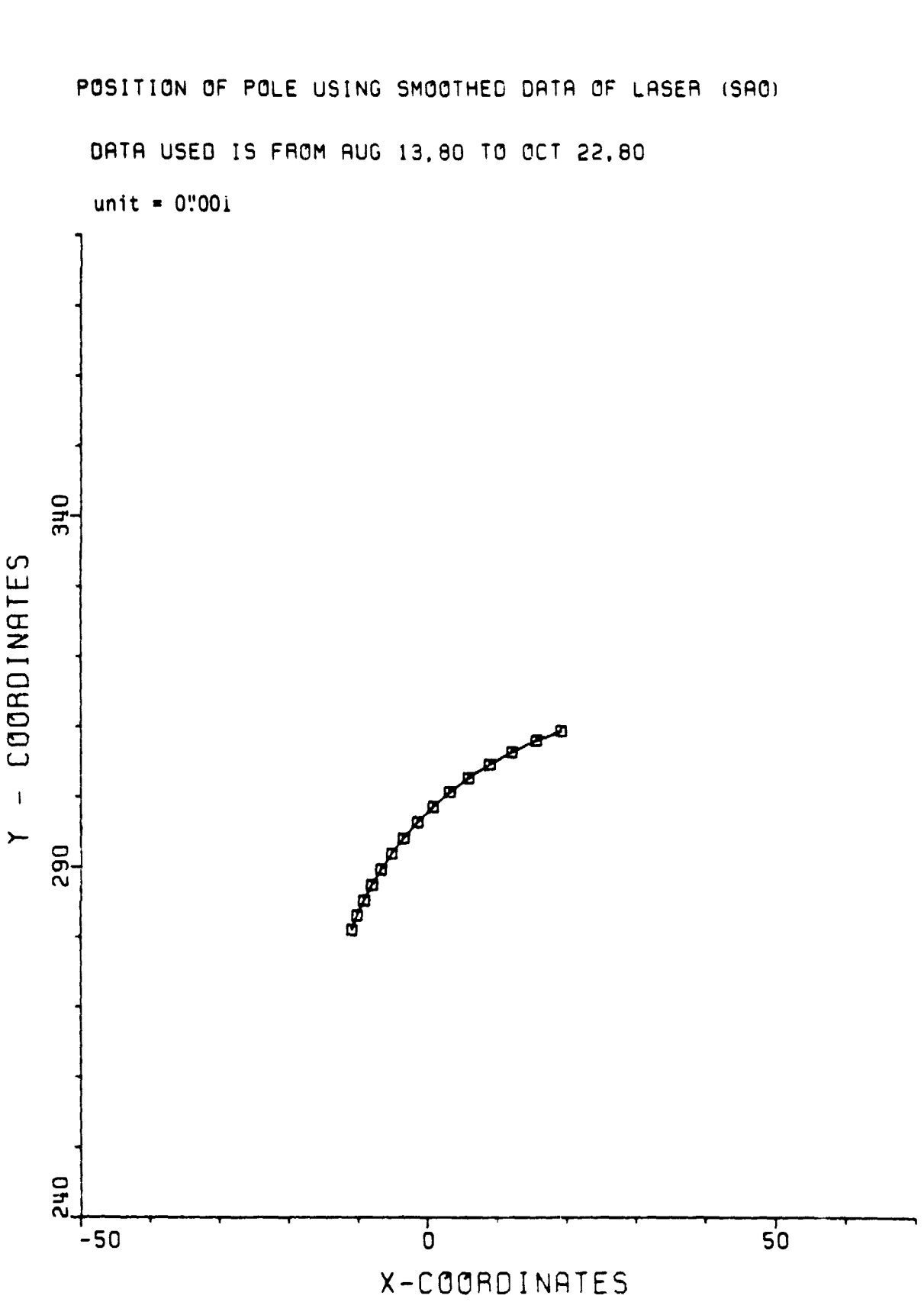
POSITION OF POLE USING SMOOTHED DATA OF LASER (SAO)
DATA USED IS FROM AUG 13,80 TO OCT 22,80
unit = 0".001
Y - COORDINATES
340
290
240
-50
0
50
X-COORDINATES

Fig. 4

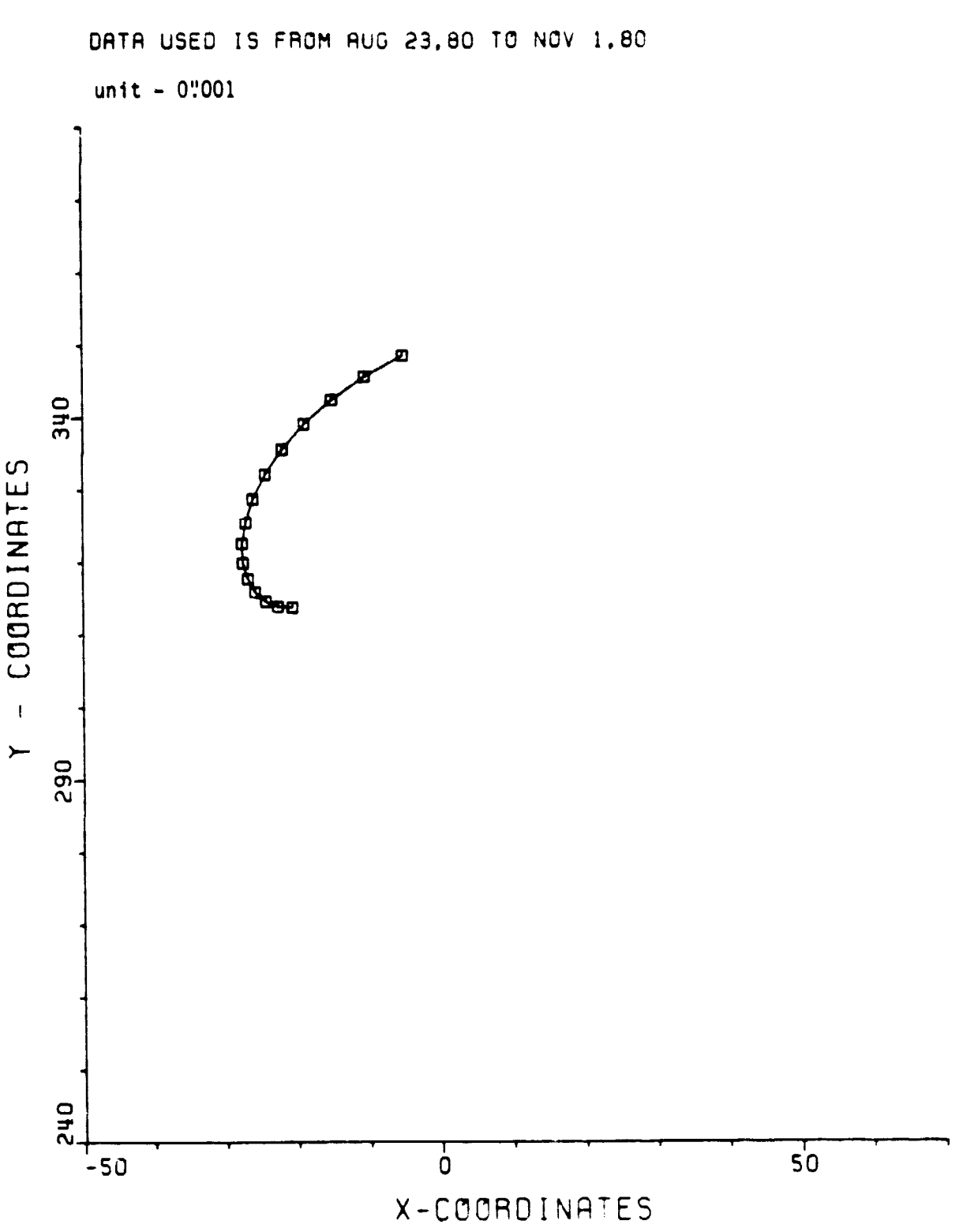
POSITION OF POLE USING SMOOTHED DATA OF LASER (NASA)
DATA USED IS FROM AUG 23,80 TO NOV 1,80
unit - 0".001
Y - COORDINATES
340
290
240
-50
0
50
X-COORDINATES

Fig. 5

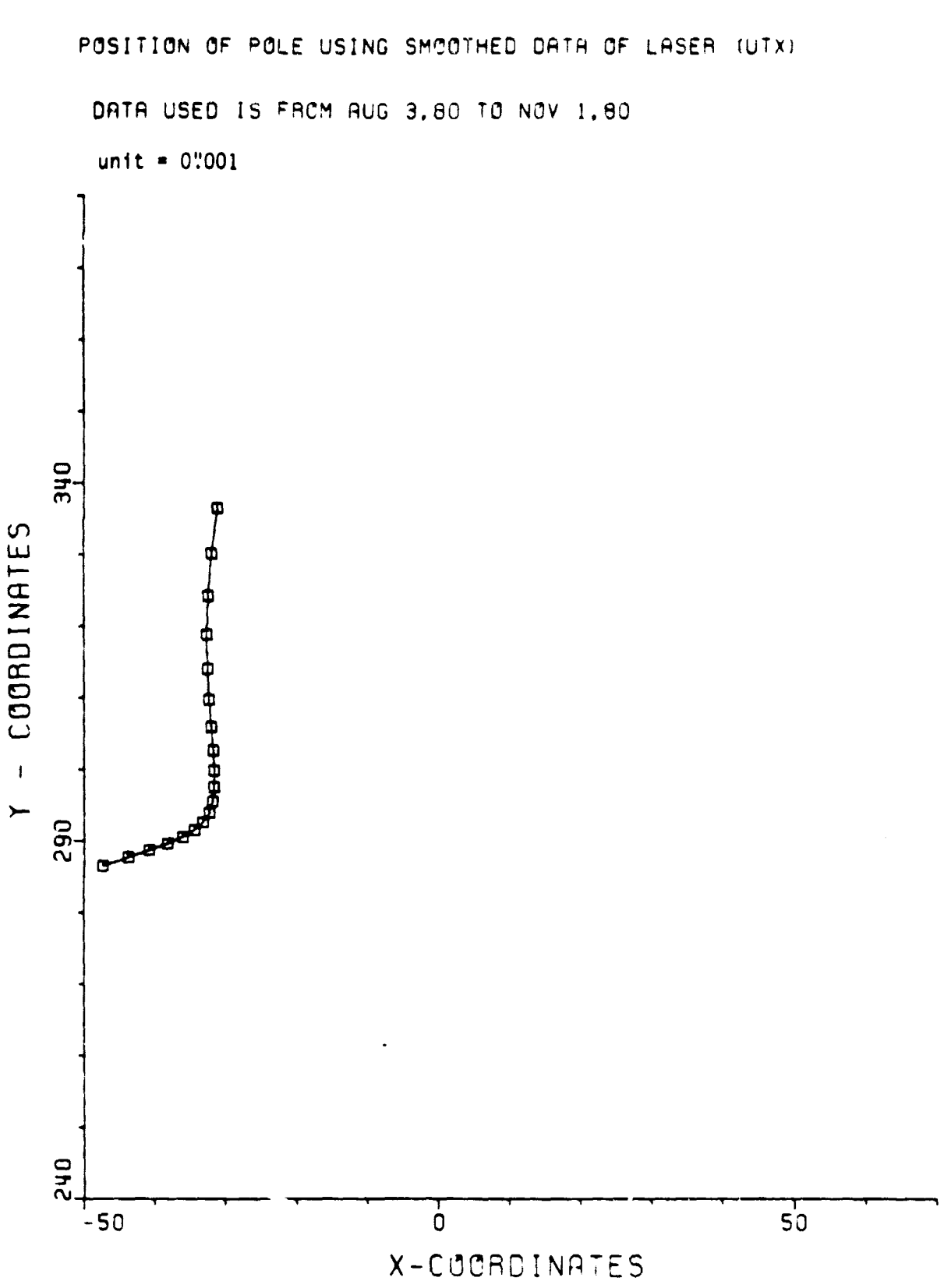
POSITION OF POLE USING SMOOTHED DATA OF LASER (UTX)
DATA USED IS FROM AUG 3,80 TO NOV 1,80
unit = 0".001
Y - COORDINATES
340
290
240
-50
0
50
X-COORDINATES

Fig. 6

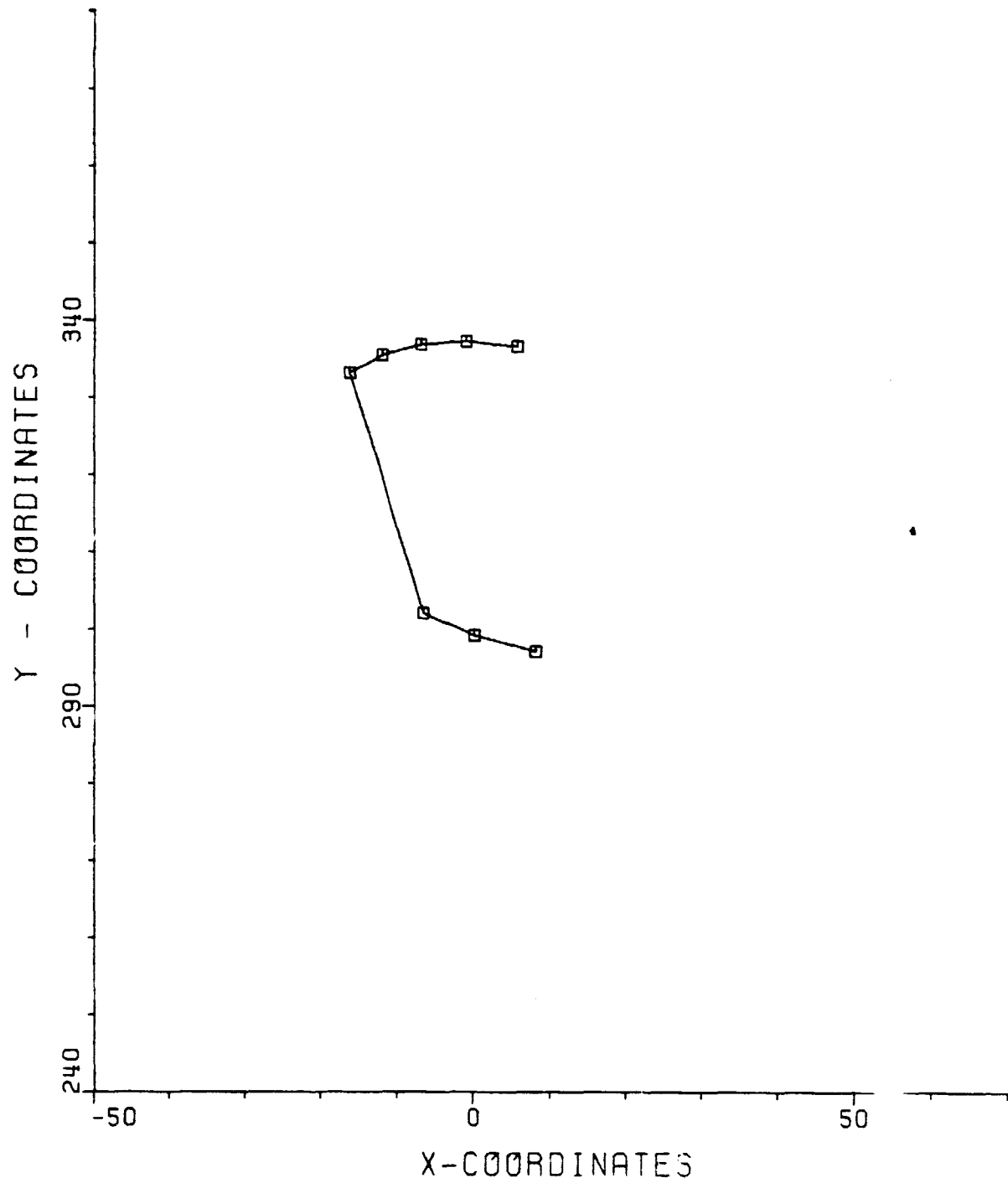
POSITION OF POLE USING SMOOTHED DATA OF LASER (CNS)
DATA USED IS FROM AUG 3,80 TO OCT 12,80
unit = 0".001
Y - COORDINATES
340
290
240
-50
0
50
X-COORDINATES

Fig. 7

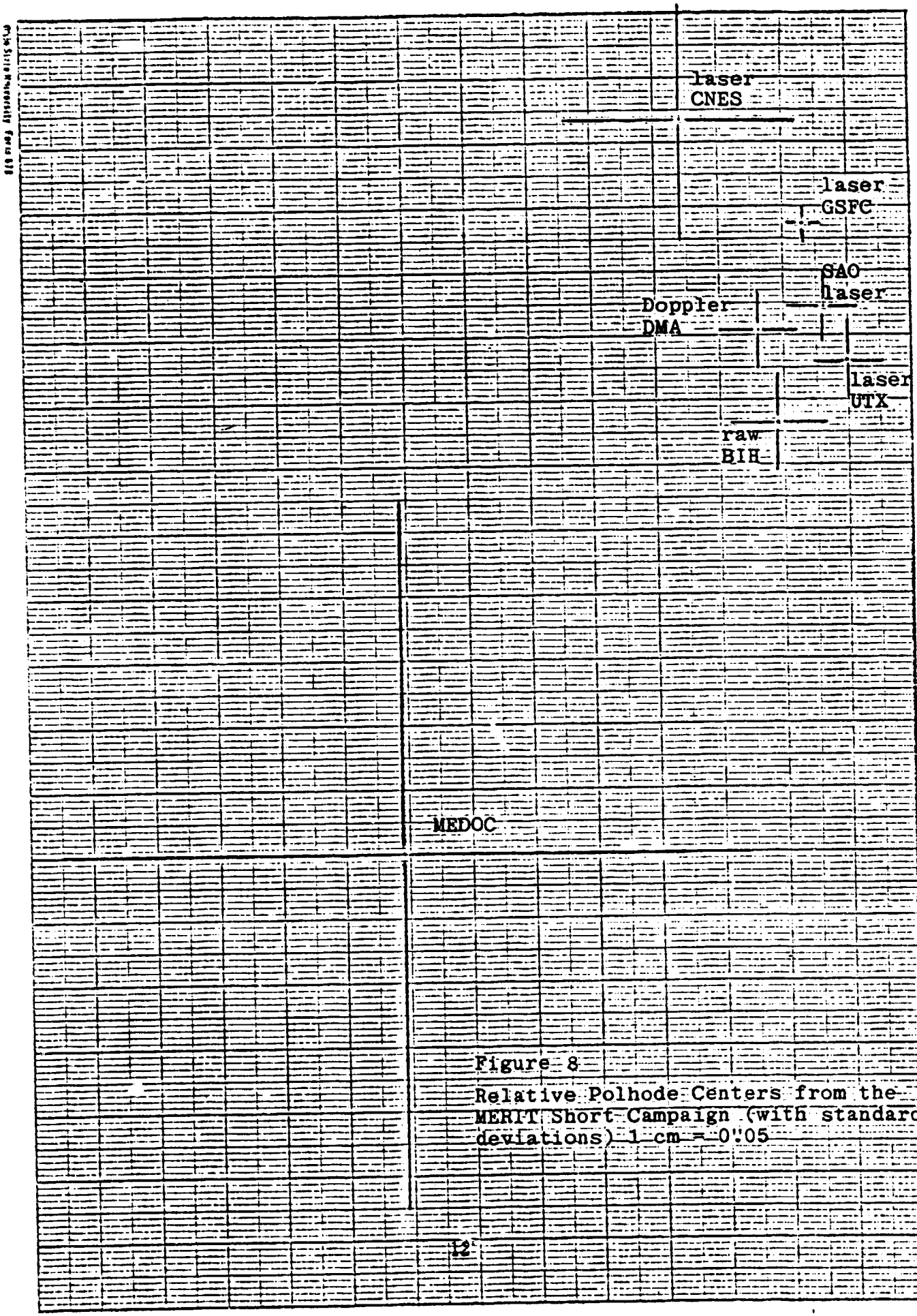

Figure 8

Relative Polhode Centers from the MERIT Short Campaign (with standard deviations) 1 cm = 0".05

2.2 VLBI Investigations - On the Time Delay Weight Matrix in VLBI Geodetic Parameter Estimation

2.21 Introduction

A VLBI baseline consists of two antennas simultaneously observing the random signals emitted from an extragalactic radio source. The reception of the signal at one antenna is delayed in time from its reception at the other antenna due to the difference in path length that the signal must travel. Denoting the time delay by τ_{ij} we have

$$\tau_{ij} = t_j - t_i$$

where t_i (t_j) is the time of arrival at station i (j). For a set of time delay observations about a triangle of stations we have τ_{12}, τ_{13} and τ_{23}. Assuming that we were able to directly measure the times of arrival of the signal at each antenna (with equal precision) then it can easily be shown [Bock, 1980] that the unscaled variance-covariance matrix for that set of time delays is given by

$$\tau_{ij} = \begin{bmatrix} 1 & \frac{1}{2} & -\frac{1}{2} \\ \frac{1}{2} & 1 & \frac{1}{2} \\ -\frac{1}{2} & \frac{1}{2} & 1 \end{bmatrix}$$

Since the determinant of this matrix is zero, the three time delays in this ideal case are seen to be linearly dependent being related by

$$\tau_{12} + \tau_{23} = \tau_{13}$$

Therefore, for each set of observations from a triangle of stations, one time delay would be redundant, and, furthermore, any two time delays would be correlated by a factor of $\frac{1}{2}$. However, in reality, the time delays are not estimated in this manner but are the result of a complex estimation procedure [Whitney, 1974; Whitney et al., 1976] whose first step is the cross-correlation of the signals recorded on magnetic tape. In order to estimate, for instance, the pair τ_{12} and τ_{13}, the signals from station 1 are correlated with both the signals from station 2 and the signals from station 3; the station 1 signals, therefore, are involved in both cross-

correlations. The focus of this investigation is to assess the magnitude of the correlation between the cross-correlations on two baselines with a common station when all observations are performed simultaneously. If there is an indication of significant correlation (obviously the correlation will lie between 0 and ½), the weight matrix for time delays used in the least squares estimation of geodetic parameters must be modified accordingly (in VLBI work today the weight matrix is assumed to be diagonal). See [Bock, 1980] for simulations on the effect of correlations on parameter precision estimates. The goal of centimeter accuracy in baseline determination for the detection of, for example, plate tectonic motion is the rationale behind this study, i.e., all possible modeling errors need to be investigated.

This is a shortened and modified version of the final report to be presented at a later time.

2.22 Group Delay Estimation and Statistics

This very brief review of the measurement process is given through to the estimation of group delay (which is the estimate of the time delay so-called due to the fact that its estimation involves observations over a band of frequencies). The signal is collected at each antenna (as a voltage --see the discussion below on the statistical model), passed through the receiver chain where it is corrupted by noise. The receiver chain includes a radio frequency amplifier which increases the power of the signal, followed by mixing the signal with a strong local oscillator signal, generated by a hydrogen maser, to convert the signal to an intermediate frequency. The resulting signal is again amplified and distributed at 28 narrow bands of 2 mHz width [Rogers, 1979]. At this point the new video frequency signals in each channel are in analog form. The signals are clipped, sampled at the Nyquist rate, formatted and recorded on magnetic tape along with accurate timing codes. The clipping can be represented as a function which normalizes the amplitude of the signal voltage, X(t) such that [Thomas, 1976]

$$F(X(t)) = \pm 1 \text{ if } |X(T)| > 0$$
$$F(X(t)) = -1 \text{ if } |X(T)| < 0$$

The recorded signals are thus recorded in digital form.

The signal $x_2(t)$ received at the second station is equivalent to the signal $x_2(t)$ received at the first station but delayed in time by τ_{12} such that

$$x_2(t) = x_1(t - \tau_{12})$$

The Fourier transform of $x_2(t)$ yields in the frequency domain

$$x_2(\omega) = \int_{-\infty}^{\infty} x_2(t)\, e^{-i\omega t}\, dt = x_1(\omega)\, e^{-i\omega\tau_{12}}$$

where ω is the radio frequency.

It has been demonstrated by [Rogers, 1970] and [Whitney, 1974] that the maximum likelihood estimate of (group) delay and delay rate (the time derivative of delay) can be obtained by maximizing the counter-rotated cross-spectrum (as defined in [Whitney, 1974]) summed over BT components where B is the channel bandwidth and T the total integration time, as

$$\max_{\tilde{\tau}_{12},\dot{\tilde{\tau}}_{12},\tilde{\phi}_{12}} \text{ over } \sum_{\omega} X_1(\omega)\, X_2^*(\omega)\, e^{-i[\omega(\tilde{\tau}_{12} + \dot{\tilde{\tau}}_{12}t) + \tilde{\phi}_{12}]}$$

where $\tilde{\tau}_{12}$, $\dot{\tilde{\tau}}_{12}$, $\tilde{\phi}_{12}$ are trial delay, delay rate and fringe phase based on the best a priori information available, and ω is now the video frequency. The maximization above is equivalent to the cross-correlation of the signals recorded at both stations with fringe rotation, that is, shifting one-bit stream, on the basis of a priori information, in order to align the two-bit streams to a point of near-maximum correlation, followed by multiplication of the signals. That the above expression represents a cross-correlation follows from the convolution theorem of Fourier analysis (see, for example, [Bath, 1974]) which states that if

$$f_1(t) \longleftrightarrow F_1(\omega) \text{ and } F_2(t) \longleftrightarrow F_2(\omega)$$

then

$$f_1(t) \circledast f_2(t) \longleftrightarrow f_1(\omega)\, f_2(\omega)$$

That is, convolution (symbolized by $\circledast$) in the time domain is equivalent to multiplication in the frequency domain. Convolution is defined by

$$f_1(t) \circledast f_2(t) = \int_{-\infty}^{\infty} f_1(\tau)\, f_2(t-\tau)d\tau = \int_{-\infty}^{\infty} f_1(t-\tau)\, f_2(\tau)d\tau$$

whereas cross-correlation is defined as

$$R_{f_1 f_2}(\tau) = \int_{-\infty}^{\infty} f_1(t)\, f_2(t+\tau)dt = \int_{-\infty}^{\infty} f_1(t-\tau) f_2(t)dt$$

Thus convolution is the same as cross-correlation except that one of the time series should be taken in reverse order, i.e.,

$$R_{f_1 f_2}(\tau) = f_1(-\tau) \circledast f_2(\tau)$$

where τ in the above equations refers to the familiar time lag between two time series. Algorithms designed to approximate the cross-correlation, in practice, are given in [Whitney, 1974].

An expression for the normalized analog cross-correlation function assuming that both stations possess a square bandpass filter of width W is given in [Thomas, 1972a,b and 1973] as

$$R_{12}(\tau_m) = \frac{E\{X_1(t)\, X_2(t+\tau_m)\}}{E\{X_1^2(t)\}\, E\{X_2^2(t)\}} = \left[\gamma_{12} \frac{T_{A_1}\, T_{A_2}}{(T_{A_1} + T_{R_1})(T_{A_2} + T_{R_2})} \frac{W_D}{W} \right] \cdot \frac{\sin\left[\pi W_D\, \Delta\tau_{12}\right]}{\pi W_D\, \Delta\tau_{12}} \cos\phi_{f_{12}}$$

where τ_m is the model delay by which the signals are shifted in order to bring the data streams at both stations in close alignment. The expression in brackets is the amplitude of the cross-correlation function for an extended source (a source that subtends a finite solid angle as opposed to a point source). The fringe visibility γ accounts for the power lost due to self-interference of the extended source (γ=1 for a point source); W_D/W accounts for power lost due to imperfect bandpass alignment; the ratio of antenna temperatures T_{A_1} and T_{A_2} and receiver temperatures T_{R_1}, T_{R_2} described in the next section account for signal-to-noise properties. The $\frac{\sin x}{x}$ function indicates the accuracy with which the two signal streams have been aligned and peaks for $\Delta\tau = \tau - \tau_m = 0$, τ being the true time delay (including atmospheric and instrumental delays as well as the purely geometric delay). The so-called fast fringes $\cos\phi_f$ expresses the overall phase behavior of the cross-correlated signals. For digital signals, in the case when the correlation amplitude is small ($\sim$ 0.001 - 0.1) as is the case in

VLBI work today, the digital cross-correlation function has a further loss of $2/\pi$ in correlation amplitude (see [Thomas, 1972b] also for the strong signal case).

Once optimal values for delay and delay rate have been determined (for each frequency channel), the fringe phase (the phase difference) for the same frequency channel at stations 1 and 2 can be estimated by [Whitney, 1974]

$$\tan \hat{\phi}_{12} = \frac{\mathrm{Im}\left\{\sum_{\omega} S_{12}(\omega)\right\}}{\mathrm{Re}\left\{\sum_{\omega} S_{12}(\omega)\right\}}$$

where $S_{12}(\omega)$ is the counter-rotated cross-sprectrum above using the optimal values of delay and delay rate for one channel. (Im is the imaginary part, Re the real part of the summations which are complex quantities.)

In the bandwidth synthesis technique [Rogers, 1970, Whitney et al., 1976], the fringe phase is determined over several frequency channels (spanning a total bandwidth of up to 400 mHz in the Mark III system) in order to improve the accuracy of group delay (and delay rate) estimation, and to resolve 2π ambiguities in the fringe phase. The final estimate of group delay is the slope of a line passed in the least squares sense through the estimated phases of several frequency channels [Whitney, 1974]. The frequency channels are not generally uniformly spaced across the total bandwidth. Suppose we have observed a radio source from three stations, and that fringe phases have been estimated over n channels identical on each of the three baselines. Further suppose that the full variance-covariance matrix for the estimated phases over all channels is available. We shall assume that it takes on the following block-diagonal form

$$\Sigma_{\phi} = \begin{bmatrix} \Sigma_{\phi_1} & & & 0 \\ & \Sigma_{\phi_2} & & \\ & & \ddots & \\ 0 & & & \Sigma_{\phi_n} \end{bmatrix}_{3n \times 3n}$$

where

$$\Sigma_{\phi_1} = \begin{bmatrix} \sigma^2_{\phi_{12}} & \sigma_{\phi_{12},\phi_{13}} & \sigma_{\phi_{12},\phi_{23}} \\ & \sigma^2_{\phi_{13}} & \sigma_{\phi_{13},\phi_{23}} \\ \text{sym} & & \sigma^2_{\phi_{23}} \end{bmatrix}$$

Let us represent

$$P_i = \Sigma^{-1}_{\phi_i} = \begin{bmatrix} p_{11} & p_{12} & p_{13} \\ & p_{22} & p_{23} \\ \text{sym} & & p_{33} \end{bmatrix}_i ; \quad (P = \Sigma^{-1}_{\phi}, \text{ also block diagonal})$$

We have assumed that all fringe phases for one baseline (ij) have equal variances and are uncorrelated, though for each channel (observed simultaneously by all three stations) the fringe phases are correlated. The group delays as mentioned above are estimated as the slope of phase versus frequency. We shall assume that the spacing of the frequency channels is large compared to the bandwidth of a single channel so that only the spacings between the frequency channels need to be considered [Whitney, 1974]. In order to determine the correlations between sets of time delays from three baselines we use the (linear) mathematical model of a line passed through the points (ω_k, ϕ_{ijk}). ω_k refers to the video frequency of the k^{th} channel, ϕ_{ijk} the fringe phase on baseline ij, channel k. We form three sets of observation equations, one for each baseline

$$\phi_{12_k} + v_{12_k} = \tau_{12}\omega_k + b_{12}$$
$$\phi_{13_k} + v_{13_k} = \tau_{13}\omega_k + b_{13}$$
$$\phi_{23_k} + v_{23_k} = \tau_{23}\omega_k + b_{23}$$

The parameters include τ_{12}, τ_{13}, τ_{23}, the group delays to be estimated over all frequency channels and the b_{ij}, the line intercepts which for this discussion can be regarded as nuisance parameters. The v_{ijk} are observation residuals. We can write the above equations in matrix form as [Uotila, 1967]

$$V = A X - L$$

where

$$A = \begin{bmatrix} A_1 & A_2 & 0 & 0 & 0 & 0 \\ 0 & 0 & A_1 & A_2 & 0 & 0 \\ 0 & 0 & 0 & 0 & A_1 & A_2 \end{bmatrix}_{3n \times 6}$$

$$A_1 = \begin{bmatrix} \omega_1 \\ \omega_2 \\ \vdots \\ \omega_k \end{bmatrix}_{n \times 1} \quad ; \quad A_2 = \begin{bmatrix} 1 \\ \vdots \\ 1 \end{bmatrix}_{n \times 1}$$

$$L = \begin{bmatrix} \phi_{12_1} \\ \vdots \\ \phi_{12_n} \\ \phi_{13_1} \\ \vdots \\ \phi_{13_n} \\ \phi_{23_1} \\ \vdots \\ \phi_{23_n} \end{bmatrix}_{3n \times 1} \qquad X = \begin{bmatrix} \tau_{12} \\ b_{12} \\ \tau_{13} \\ b_{13} \\ \tau_{23} \\ b_{23} \end{bmatrix}_{6 \times 1}$$

The least squares solution vector for the estimated parameters is given by

$$\hat{X} = (A^T P A)^{-1} A^T P L$$

In this discussion we are only interested in the variance-covariance matrix of the parameters (assume unscaled)

$$\Sigma_{\hat{X}} = (A^T P A)^{-1}$$

where the weight matrix P has been defined above. Performing the matrix multiplication we arrive at

$$\hat{\Sigma}_X = \begin{bmatrix} \Sigma\omega_k^2 p_{11} & \Sigma\omega_k p_{11} & \Sigma\omega_k^2 p_{12} & \Sigma\omega_k p_{12} & \Sigma\omega_k^2 p_{13} & \Sigma\omega_k p_{13} \\ & \Sigma p_{11} & \Sigma\omega_k p_{12} & \Sigma\ p_{12} & \Sigma\omega_k p_{13} & \Sigma\ p_{13} \\ & & \Sigma\omega_k^2 p_{22} & \Sigma\omega_k p_{22} & \Sigma\omega_k^2 p_{23} & \Sigma\omega_k p_{23} \\ & & & \Sigma p_{22} & \Sigma\omega_k p_{23} & \Sigma p_{23} \\ & & & & \Sigma\omega_k^2 p_{23} & \Sigma\omega_k p_{33} \\ & \text{sym} & & & & \Sigma p_{33} \end{bmatrix}^{-1}$$

The $\hat{\Sigma}_\tau$ portion can be picked out after inversion including the time delay correlations.

In the case of only two frequency channels ω_1, ω_2 (say, for example, the two outermost channels (see discussion in [Thomas, 1973]), the group delay portion of the above $\hat{\Sigma}_X$ matrix reduces to

$$\hat{\Sigma}_\tau = \frac{1}{(\omega_2-\omega_1)^2} \begin{bmatrix} \sum_{k=1}^{2} \sigma^2_{\phi_{12_k}} & \sum_{k=1}^{2} \sigma_{\phi_{12_k},\phi_{13_k}} & \sum_{k=1}^{2} \sigma_{\phi_{12_k},\phi_{23_k}} \\ & \sum_{k=1}^{2} \sigma^2_{\phi_{13_k}} & \sum_{k=1}^{2} \sigma_{\phi_{13_k},\phi_{23_k}} \\ \text{sym} & & \sum_{k=1}^{2} \sigma^2_{\phi_{23_k}} \end{bmatrix}$$

In the cases where the fringe phases from channel i for all three baselines are uncorrelated, i.e.,

$$p_{11} = \frac{1}{\sigma^2_{12}} \; ; \quad p_{22} = \frac{1}{\sigma^2_{13}} \; ; \quad p_{33} = \frac{1}{\sigma^2_{23}} \; ; \quad p_{ij} = 0 \; (i \neq j)$$

the group delays are obviously also uncorrelated. In this case the variance of $\sigma^2_{\tau_{12}}$, for example, can be determined from the first block of the now block diagonal $\hat{\Sigma}_X$ matrix as

$$\Sigma_{\hat{\chi}_1} = \sigma^2_{\phi_{12}} \begin{bmatrix} \Sigma\omega_k^2 & \Sigma\omega_k \\ \Sigma\omega_k & n \end{bmatrix}^{-1}$$

which reduces for the time delay τ_{12}

$$\sigma^2_{\tau_{12}} = \frac{\sigma^2_{\phi_{12}}}{\Sigma(\omega_i - \bar{\omega})^2} \quad ; \quad \bar{\omega} = \frac{\sum_{i=1}^{n} \omega_k}{n}$$

in agreement with [Whitney, 1974] and [Thomas, 1976]. An expression for $\sigma^2_{\phi_{ij}}$ is derived in [Whitney, 1974] (for $T_A << T_R$)

$$\sigma^2_{\phi_{ij}} = \frac{T_{R_i} T_{A_j} + T_{A_i} T_{R_j} + T_{R_i} T_{R_j}}{T_{A_i} T_{A_j}} \frac{1}{2BT}$$

where the notation has been explained previously. Furthermore, he defines the signal-to-noise ratio as

$$SNR_{ij} = \rho_0 \sqrt{2BT}$$

where ρ_0 is the amplitude of the cross-correlation function described earlier (here given for an analog signal and a point source) and thus

$$\sigma^2_{\phi_{ij}} = \frac{1}{SNR_{ij}}$$

2.23 The Nature of Signal and Noise in VLBI Observations

As in all statistical detection problems, we are interested in the reception of a signal which bears information of value and noise which opposes our efforts to extract it. (This paragraph will draw from [Steinberg, 1963; and Kraus, 1966]). In radio astronomy both the signal and noise are of an equivalent statistical nature. Consider a resistance of R ohms at a temperature T (°K). The thermal agitation of the electrons in the resistor produces a voltage $n_e(t)$ at the terminals with zero mean, $E[n_e(t)] = 0$ and a flat spectrum $Sn_e(\omega) = 2kTR$ (k is Boltzman's constant). This so-called thermal or background noise can be shown experimentally to be a normal process. A resistance R is therefore equivalent to a source of voltage with zero mean and power, 2kTR in series with a noiseless resistor R. If such a voltage source is connected to an external load resistance R_L, it will deliver a certain power to it which will be maximum if the load resistence is equal to that of the source. The power delivered will be equal to kT. The voltages involved in VLBI antennas are of the same statistical nature as background noise. The same noise power is available at the terminals of an antenna (kT). The antenna has a radiation resistance R and is exposed to a sky temperature, T. Therefore, we see that observations in radio astronomy consist of the measurement of an antenna temperature and the conversion of that temperature to a measure of power received from the source. The signals are corrupted by noise as they pass through the receiver components primarily at the first stage of amplification [Thomas, 1976]. This noise is basically background noise as described above. Thus, signal and noise in VLBI observations have similar statistical properties, being modeled by the thermal noise of a resistance raised to a certain temperature. The receiver noise is expressed in terms of the radiation resistance of the antenna. It is the temperature to which the radiation resistance of the antenna would have to be raised in order to produce the same noise power as the complete receiver. The sum of antenna temperature, T_A, and the receiver temperature, T_R, is called the system temperature. Thus, the overall noise power is given by $k(T_A+T_R)$. In order to appreciate the temperatures involved, for the Mark III wideband receiver and a 10 Jansky source (1 Jansky = 10^{-26} watts/m Hz) for the Westford 18 m

antenna, T_A = 0°.45 K and for the 4 m portable antenna, T_A = 0°.03 K. The system temperature, on the other hand, is about 160° K [Rogers, 1979]. Even for large antennas observing strong extragalactic sources, the temperature will not usually exceed 1° K. Thus, antenna temperature is about two orders of magnitude smaller than receiver temperature. The signal is thus proportional to antenna temperature and the noise to receiver temperature. In order for the signal to be detected, measurements must be integrated over several minutes of time and the spanned bandwidth increased (up to 400 mHz with the Mark III receiver).

Considering the statistical nature of signal and noise in VLBI observations, it is reasonable to assign the following statistical model for the output voltage of the receiver as [Rogers, 1970]

$$X(t) = (T_A)^{\frac{1}{2}}\, s(t) + (T_R)^{\frac{1}{2}}\, n(t)$$

where s(t) is the noise signal collected by the antenna from the radio source emission and n(t) is the receiver noise. The temperatures T_A and T_R, therefore, serve as weighting factors.

The signal and noise are complex quantities whose real and imaginary parts are assumed to be normally distributed (N (0,½)), for a particular t, and independent [Whitney, 1974]. Therefore (and similarly for n(t))

$$E\{s(t)\} = E\{s_r(t) + i\, s_i(t)\} = E\{s_r(t)\} + i\{s_i(t)\} = 0$$

$$\text{var}[s(t)] = E\{|s(t)|^2\} = E\{s_r^2(t) + s_i^2(t)\} = E\{s_r^2(t)\} + E\{s_i^2(t)\} = \tfrac{1}{2}+\tfrac{1}{2}=1$$

$$\text{cov}[s(t),n(t)] = E\{s(t)\, n^*(t)\} - E\{s(t)\}\, E\{n^*(t)\} = E\{s(t)\, n^*(t)\}$$

$$= E\{s_r(t)\, n_r(t)\} + E\{s_i(t)\, n_i(t)\} + i[E\{s_i(t)\, n_r(t)\} - E\{s_r(t)\, n_i(t)\}] = 0$$

and the signal and noise are seen to be independent standard normal, N(0,1) random variables for fixed t. Both s(t) and n(t) are assumed to be stationary random processes (see [Swanson and Mathur, 1968]) so that their respective autocorrelations are a function of time difference and independent of time origin.

Since an observation is integrated over a certain time interval T and a spanned bandwidth B, s(t) and n(t) can be represented over T by

a Fourier series expansion with BT independent components. Furthermore, since the signal X(t) is generally received from an extended source, we can assume that only the correlated part of the signal contributes to the antenna temperature and the remainder contributes to the receiver temperature [Rogers, 1970].

The statistical model can just as well be written in the frequency domain as [Whitney, 1974]

$$X(\omega) = (T_A)^{\frac{1}{2}}\, s(\omega) + (T_R)^{\frac{1}{2}}\, n(\omega)$$

Both signal and noise are bandlimited which means that their spectra equal zero outside certain regions of the frequency ω [Papoulis, 1965]. The consequence of the above assumptions is that the output voltage of the receiver X(t) at each station is itself a stationary, normal (with zero mean), bandlimited stochastic process.

2.24 Correlation Analysis

We are now in a position to assess the degree of correlation between the cross-correlation of signals on any two baselines when the signals from one station are common to both processes. We shall investigate a triangle of stations observing a radio source simultaneously(since this is the basic unit for such an analysis) whose signals are represented statistically in the frequency domain as

$$X_1(\omega) = (T_{A_1})^{\frac{1}{2}}\, s_1(\omega) + (T_{R_1})^{\frac{1}{2}}\, n_1(\omega)$$
$$X_2(\omega) = (T_{A_2})^{\frac{1}{2}}\, s_2(\omega) + (T_{R_2})^{\frac{1}{2}}\, n_2(\omega)$$
$$X_3(\omega) = (T_{A_3})^{\frac{1}{2}}\, s_3(\omega) + (T_{R_3})^{\frac{1}{2}}\, n_3(\omega)$$

where

$$s_2(\omega) = s_1(\omega)\, e^{-i[\omega(\tau_{12} + \dot{\tau}_{12}t) + \phi_{12})]}$$
$$s_3(\omega) = s_1(\omega)\, e^{-i[\omega(\tau_{13} + \dot{\tau}_{13}t) + \phi_{13})]}$$

The notation is the same as in the previous section. In addition, we assume that the noise introduced at each receiver is uncorrelated with that of another receiver, i.e.,

$$E\{n_i n_j\} = 0 \text{ (and } E\{s_i n_j\} = 0) \quad (i \neq j)$$

We shall determine the degree of correlation between the cross-correlation on baseline 1-2 and 1-3. The rotated video cross-spectrum for baseline 1-2 and baseline 1-3 can be written as

$$S_{12}(\omega) = X_1(\omega)\, X_2^*(\omega)\, e^{-i\omega(\tau_{12} + \dot{\tau}_{12}t)}$$

$$S_{13}(\omega) = X_1(\omega)\, X_3^*(\omega)\, e^{-i\omega(\tau_{13} + \dot{\tau}_{13}t)}$$

which can be written in terms of signal and noise as

$$S_{12}(\omega) = \sqrt{T_{A_1} T_{A_2}}\, s_1(\omega)\, s_1^*(\omega)\, e^{i\phi_{12}} + \sqrt{T_{R_1} T_{A_2}}\, n_1(\omega)\, s_1^*(\omega)\, e^{i\phi_{12}} + \sqrt{T_{A_1} T_{R_3}}\, s_1(\omega)\, n_2'^*(\omega) + \sqrt{T_{R_1} T_{R_2}}\, n_1(\omega)\, n_2'^*(\omega)$$

$$S_{13}(\omega) = \sqrt{T_{A_1} T_{A_3}}\, s_1(\omega)\, s_1^*(\omega)\, e^{i\phi_{13}} + \sqrt{T_{R_1} T_{A_3}}\, n_1(\omega)\, s_1^*(\omega)\, e^{i\phi_{13}} + \sqrt{T_{A_1} T_{R_3}}\, s_1(\omega)\, n_3'^*(\omega) + \sqrt{T_{R_1} T_{R_3}}\, n_1(\omega)\, n_3'^*(\omega)$$

where

$$n_2'^*(\omega) = n_2(\omega)\, e^{i\omega(\tau_{12} + \dot{\tau}_{12}t)}$$

$$n_3'^*(\omega) = n_3(\omega)\, e^{i\omega(\tau_{13} + \dot{\tau}_{13}t)}$$

We shall assume as in [Whitney, 1974] that $n_2'(\omega)$ has the same statistics as $n_2(\omega)$ and likewise for $n_3'(\omega)$ and $n_3(\omega)$.

The above $S_{12}(\omega)$ and $S_{13}(\omega)$ are evaluated as the sum over a large number of independent short time intervals spanning an observation and refer to one component in the observed frequency spectrum. The maximization, as mentioned before, is performed by summation over BT independent points in the frequency spectrum. We can represent this summation as in [Whitney, 1974] by

$$\vec{R}_{12} = \Sigma X_1(\omega)\, X_2^*(\omega)\, e^{-i\omega(\tau_{12} + \dot{\tau}_{12}t)} = \sqrt{T_{A_1} T_{A_2}}\, e^{i\phi_{12}}\, \Sigma s_1(\omega)\, s^*(\omega) + \sqrt{T_{R_1} T_{A_2}}\, e^{i\phi_{12}}\, \Sigma n_1(\omega)\, s^*(\omega) + \sqrt{T_{A_1} T_{R_2}}\, \Sigma s(\omega)\, n_2'^*(\omega) + \sqrt{T_{R_1} T_{R_2}}\, \Sigma n_1(\omega)\, n_2'^*(\omega)$$

and

$$\vec{R}_{13} = \Sigma X_1(\omega)\, X_3^*(\omega)\, e^{-i\omega(\tau_{13} + \dot{\tau}_{13}t)}$$

$$= \sqrt{T_{A_1} T_{A_3}}\, e^{i\phi_{13}}\, \Sigma s(\omega)\, s^*(\omega) + \sqrt{T_{R_1} T_{A_3}}\, e^{i\phi_{13}}\, \Sigma n_1(\omega)\, s^*(\omega)$$

$$+ \sqrt{T_{A_1} T_{R_3}}\, \Sigma s(\omega)\, n_3'^*(\omega) + \sqrt{T_{R_1} T_{R_3}}\, \Sigma n_1(\omega)\, n_3'^*(\omega)$$

where we have dropped the subscript from the signal terms. We are only concerned with the observations that are common to all three stations. It can be shown easily that all the terms in the expressions S_{12} and S_{13} are independent of each other and the real and imaginary parts of each term are independent [Whitney, 1974]. Thus, $\vec{R}_{12}$ and $\vec{R}_{13}$ are vectors in the complex plane, and are the sums of independent random variables.

The correlation between these two cross-correlation processes given by $\vec{R}_{12}$ and $\vec{R}_{13}$ can be defined as

$$\vec{\rho} = \frac{\mathrm{cov}[\vec{R}_{12}, \vec{R}_{13}]}{\{\mathrm{var}[\vec{R}_{12}]\ \mathrm{var}[\vec{R}_{13}]\}^{\frac{1}{2}}}$$

which is also a vector in the complex plane since in general the covariance between two complex random variables (in our case, the sume of uncorrelated random variables) is complex but the variance is real [Jenkins and Watts, 1968]. For the covariance between $\vec{R}_{12}$ and $\vec{R}_{13}$, by definition [Papoulis, 1965],

$$\mathrm{cov}[\vec{R}_{12}, \vec{R}_{13}] = E\{[\vec{R}_{12} - E\{\vec{R}_{12}\}][\vec{R}_{13}^* - E\{\vec{R}_{13}^*\}]\}$$

$$= E\{\vec{R}_{12}\, \vec{R}_{13}^*\} - E\{\vec{R}_{12}\}\, E\{\vec{R}_{13}^*\}$$

$$= (BT)\, (T_{A_1} + T_{R_1})\, \sqrt{T_{A_2} T_{A_3}}\, e^{i(\phi_{12} - \phi_{13})}$$

where the derivation is given in the final report. To derive an expression for the variances we can use the property that the four terms of both $\vec{R}_{12}$ and $\vec{R}_{13}$ are independent and therefore the variances of each term can be summed. By definition [Papoulis, 1965]

$$\sigma^2_{\vec{R}_{12}} = E\{|\vec{R}_{12} - E\{\vec{R}_{12}\}|^2\}$$

$$= (BT)(T_{A_1} + T_{R_1})(T_{A_2} + T_{R_2})$$

and

$$\sigma^2_{\vec{R}_{13}} = E\{|\vec{R}_{13} - E\{\vec{R}_{13}\}|^2\}$$

$$= (BT)(T_{A_1} + T_{R_1})(T_{A_3} + T_{R_3})$$

where the derivations are given in the final report. Then, for the correlation vector

$$\vec{\rho}_{\vec{R}_{12},\vec{R}_{13}} = \sqrt{\frac{T_{A_2} T_{A_3}}{(T_{A_2} + T_{R_2})(T_{A_3} + T_{R_3})}}\; e^{i(\phi_{12} - \phi_{13})}$$

The magnitude of $\vec{\rho}_{\vec{R}_{12},\vec{R}_{13}}$,

$$|\vec{\rho}_{\vec{R}_{12},\vec{R}_{13}}| = \sqrt{\frac{T_{A_2} T_{A_3}}{(T_{A_2} + T_{R_2})(T_{A_3} + T_{R_3})}}$$

is a measure of the degree of correlation between the two cross-correlation processes, represented by $\vec{R}_{12}$ and $\vec{R}_{13}$. (The same result has been derived independently by Herring [private communication].) The argument of $\vec{\rho}_{\vec{R}_{12},\vec{R}_{13}}$

$$\arg \vec{\rho}_{\vec{R}_{12},\vec{R}_{13}} = \tan^{-1} \frac{\mathrm{Im}\, \vec{\rho}}{\mathrm{Re}\, \vec{\rho}} = \phi_{12} - \phi_{13}$$

expresses the effective phase difference between the two processes--$\phi_{12} - \phi_{13}$ is the angle between $\vec{R}_{12}$ and $\vec{R}_{13}$ in the complex plane. The magnitude of the correlation vector is defined in general by [Jenkins and Watts, 1968] as the coherence between two complex random variables, X_1 and X_2, by

$$k_{12} = \frac{|\mathrm{cov}\, [X_1, X_2^*]|}{\{\mathrm{var}\, [X_1]\, \mathrm{var}\, [X_2]\}^{\frac{1}{2}}}$$

The correlation vector is also referred to in the literature as the complex correlation factor used, for example, in optics for the study of light from an extended, incoherent quasi-monochromatic source [Born and Wolf, 1964].

Extending the above results, the following Hermitian matrix (similar to the coherency matrix in optics) for the cross-correlation of signals in a VLBI triangle can be defined as

$$J = \begin{bmatrix} \mathrm{var}\, [\vec{R}_{12}] & \mathrm{cov}\, [\vec{R}_{12},\vec{R}_{13}] & \mathrm{cov}\, [\vec{R}_{12},\vec{R}_{23}] \\ \mathrm{cov}\, [\vec{R}_{13},\vec{R}_{12}] & \mathrm{var}\, [\vec{R}_{13}] & \mathrm{cov}\, [\vec{R}_{13},\vec{R}_{23}] \\ \mathrm{cov}\, [\vec{R}_{23},\vec{R}_{12}] & \mathrm{cov}\, [\vec{R}_{23},\vec{R}_{13}] & \mathrm{var}\, [\vec{R}_{23}] \end{bmatrix} =$$

$$= \begin{bmatrix} T_{S_1}T_{S_2} & T_{S_1}\sqrt{T_{A_2}T_{A_3}}\, e^{i(\phi_{12}-\phi_{13})} & T_{S_2}\sqrt{T_{A_1}T_{A_3}}\, e^{i(\phi_{12}-\phi_{23})} \\ T_{S_1}\sqrt{T_{A_2}T_{A_3}}\, e^{-i(\phi_{12}-\phi_{13})} & T_{S_1}T_{S_3} & T_{S_3}\sqrt{T_{A_1}T_{A_2}}\, e^{i(\phi_{13}-\phi_{23})} \\ T_{S_2}\sqrt{T_{A_1}T_{A_3}}\, e^{-i(\phi_{12}-\phi_{23})} & T_{S_3}\sqrt{T_{A_1}T_{A_2}}\, e^{-i(\phi_{12}-\phi_{13})} & T_{S_2}T_{S_3} \end{bmatrix}$$

where $T_{S_j} = T_{A_j} + T_{R_j}$, the system temperature for station j.

The corresponding coherency (correlation) coefficient matrix is given by

$$C = \begin{bmatrix} 1 & |\rho_{\vec{R}_{12},\vec{R}_{13}}| & |\rho_{\vec{R}_{12},\vec{R}_{23}}| \\ & 1 & |\rho_{\vec{R}_{13},\vec{R}_{23}}| \\ & & 1 \end{bmatrix} = \begin{bmatrix} 1 & \sqrt{\frac{T_{A_2}T_{A_3}}{T_{S_2}T_{S_3}}} & \sqrt{\frac{T_{A_1}T_{A_3}}{T_{S_1}T_{S_3}}} \\ & 1 & \sqrt{\frac{T_{A_1}T_{A_2}}{T_{S_1}T_{S_2}}} \\ & & 1 \end{bmatrix}$$

where we can pick out the coherence between any two cross-correlations from the off-diagonal elements.

It is interesting to note that the coherence between the cross-correlations for any two baselines (with a common station) is just the amplitude (denoted here by $|\vec{\rho}|_{R_{jk}}$) of the normalized cross-correlation function defined earlier (or as is defined in [Whitney, 1974], the true correlation coefficient of the third baseline),i.e.,

$$|\vec{\rho}|_{\vec{R}_{ij},\vec{R}_{ik}} = |\vec{\rho}|_{\vec{R}_{jk}}$$

for the case of observations to a point source with the signals recorded in analog form.

In order to assess the magnitude of the off-diagonal elements of matrix C, i.e., the degree of coherence (correlation) between cross-correlations on two baselines with a common station, we recall from the earlier discussion that in VLBI work today $T_A \ll T_R$. This indicates that the C matrix is very nearly the identity matrix, i.e., the cross-correlation pairs are virtually uncorrelated ($|\vec{\rho}| \sim 0.001$ for the example of the previous

section). It follows that the fringe phases are uncorrelated and consequently the group delays (as well as the delay rates). In fact, the correlations can be expected to be even smaller considering that we are observing extended sources so that the correlation would have to be multiplied by a fringe visibility factor (remember $0<\gamma<1$). In addition, we know that digitizing of the signals reduces the amplitude of the cross correlation function by a factor of $2/\pi$ and (in the case of weak signals) can be expected to affect the correlations. Finally, the theoretical cross-correlation procedure as described earlier is only approximated in practice, which will also tend to reduce the degree of correlation (see [Rogers et al., 1979]).

On the other extreme, in the limiting case where $T_A = T_R$

$$C = \begin{bmatrix} 1 & \frac{1}{2} & \frac{1}{2} \\ & 1 & \frac{1}{2} \\ \text{sym} & & 1 \end{bmatrix}$$

as could be envisioned for satellite interferometry where a radio antenna (e.g., SERIES) would observe an artificial satellite transmitting a much stronger signal than extragalactic radio signals. Furthermore, the satellite could be considered a point source and digitization would not be expected to decrease the cross-correlation function amplitude (see [Thomas, 1972b]). It then could be inferred (this will be shown in the final report) that the fringe phases are correlated in the same manner. Since the C matrix in this case is singular, this implies that only two cross-correlations in a triangle are independent and likewise for the fringe phase. The covariances of the Σ_{ϕ_i} matrices defined earlier could then be formed by

$$\sigma_{\phi_{ij},\phi_{jk}} = \rho_{\phi_{ij},\phi_{jk}} \sigma_{\phi_{ij}} \sigma_{\phi_{jk}}$$

where ρ, the correlation between fringe phases will approach $\frac{1}{2}$. It is easy to see (at least in the two-channel case) that the correlations between group delays would approach that of the hypothetical situation described in the introduction and could be computed in general by the Σ_t portion of the $\Sigma_{\hat{X}}$ matrix developed in Section 2.2.2.

References

Bath, M. (1974) Spectral Analysis in Geophysics, Elsevier Scientific Publ. Co., Amsterdam, pp. 75-93.

Bock, Y. (1980) A VLBI Variance-Covariance Analysis Interactive Computer Program, MSc thesis, Dept. of Geodetic Science, Ohio State Univ, Columbus (Dept. of Geodetic Science Rept. No. 298).

Born, M. and E. Wolf (1964) Optics, Macmillan Co., New York, pp. 544-546.

Jenkins, G.M. and D.G. Watts (1968) Spectral Analysis and Its Applications, Holden-Day, San Francisco, pp. 463-4.

Kraus, J.D. (1966) Radio Astronomy, McGraw Hill, New York.

Middleton, D. (1960) An Introduction to Statistical Communication Theory, McGraw Hill, New York, p. 343.

Mood, A.M., F.A. Graybill and D.C. Boes (1974) Introduction to the Theory of Statistics, McGraw Hill, New York, pp. 178-80.

Moran, J.M. (1976) "Very Long Baseline Interferometric Observations and Data Reduction," Methods of Experimental Physics, Vol. 12, Part C, M.L. Meeks, ed., Academic Press, New York, pp. 228-260.

Papoulis, A. (1965) Probability, Random Variables, and Stochastic Processes, McGraw Hill, New York.

Rogers, A.E.E. (1979) "Microwaves to Megabits," Radio Interferometry Techniques for Geodesy, NASA Conference Publ. 2115, pp. 297-304.

Rogers, A.E.E. (1970) "Very Long Baseline Interferometry with Large Effective Bandwidth for Phase-Delay Measurements," Radio Science, 5, 10, pp. 1239-1247.

Rogers, A.E.E. and the East Coast VLBI Group (1979) "The Sensitivity of a Very Long Baseline Interferometer." Radio Interferometry Techniques for Geodesy, NASA Conference Publ. 2115, pp. 275-281.

Steinberg, J.L. and J. Lequeux (1963) Radio Astronomy, McGraw Hill, New York.

Swanson, G.W. and N.C. Mathur (1968) "The Interferometer in Radio Astronomy," Proc. of the IEEE , Vol.56, No. 12.

Thomas, J.B. (1972a) "An Analysis of Long Baseline Radio Interferometry," The Deep Space Network Technical Rept. 32-1526, VII, Jet Propulsion Lab., Pasadena, Calif., pp. 37-50.

Thomas, J.B. (1972b) "An Analysis of Long Baseline Radio Interferometry, Part II," The Deep Space Network Progress Report 32-1526, VIII, Jet Propulsion Lab., Pasadena, Calif., pp. 29-38

Thomas, J.B. (1973) "An Analysis of Long Baseline Radio Interferometry, Part III, The Deep Space Network Progress Report 32-1526, XVI, Jet Propulsion Lab., Pasadena, Calif, pp. 47-64.

Thomas, J.B. (1976) "System Noise Effects in VLBI Measurements," Engineering Memorandum 315.6, Jet Propulsion Lab., Pasadena, Calif.

Uotila, U.A. (1967) "Introduction to Adjustment Computation with Matrices," unpublished lecture notes, Dept. of Geodetic Science, Ohio State Univ., Columbus.

Whitney, A.R. (1974) Precision Geodesy and Astrometry via Very Long Baseline Interferometry, PhD Thesis, Massachusetts Inst. of Technology, Cambridge.

Whitney, A.R., A.E.E. Rogers, H.F. Hinteregger, C.A. Knight, J.I. Levine, S. Lipincott, T.A. Clark, I.I. Shapiro and D.S. Robertson (1976) "A Very-Long Baseline Interferometer System for Geodetic Applications," Radio Science, 11, 5, pp. 421-432.

2.3 Utilization of Range Difference Observations in Geodynamics

2.31 Utilization of Lageos Laser Range Differences

Introduction

The objectives of this project as originally stated in the proposal are the development and implementation of the technique of range differencing with Lageos in order to obtain more accurate estimates of baseline lengths and polar motion variations. It is expected, and the simulations done to date confirm this, that by means of differencing quasi-simultaneous range observations a great deal of orbital biases can be eliminated resulting in an estimate which is virtually bias free. In the past few months attempts were made to use real data in order to assert the conclusions made on the basis of the simulations. Partly due to the oversimplified models used in our software (GEOSPP80) and partly due to the very poor geometry and distribution of the data, these attempts fell short of providing any conclusive results. It was realized, however, that even with the best possible geometry and distribution of the observations, certain physical phenomena would have to be included in the model. This being the case, a complete revision of our software was undertaken, which resulted in a new version (GEOSPP81) currently undergoing tests. Given in the following is a brief summary of the various models implemented in the new version.

2.311 Data Preprocessing

As mentioned in previous reports, it is quite improbable, if not impossible, to obtain exactly simultaneous laser observations from two ground stations to a satellite. Modern lasers, however, have high repetition rates and given fair weather conditions and accurate predictions, a sequence of ranges at a rate of about 1 pps can be easily achieved. Since an average Lageos pass lasts about half an hour, this implies a large amount of data. The high altitude of the target makes it possible to observe it from several stations simultaneously, even if the stations' separation is of continental extent. The current procedure to obtain the quasi-simultaneous ranges from data sets such as described above is to determine the "overlap" observations for the station pairs involved, isolate these observations and

determine which of the two stations in each pair has a denser data distribution. Once this is determined, the data of the station with the most observations are fed into a cubic-spline interpolator and ranges are obtained for each of the data points in the alternate station's record. These ranges then are differenced to produce the range-difference data for GEOSPP81. The data used in this procedure have already been corrected for systematic errors (Tape-90 data in GEODYN terminology). Figs. 9 and 10 depict the data record for two passes of Lageos. The bars indicate the epochs when the actual observation occurred and the curve which joins their centers is the spline fit to these data. The stations marked with (*) are the ones for which we used the original observations in the formation of the range differences.

2.312 Reference Frames

A number of reference frames are involved depending on the phenomena being treated in the program. The integration of the orbit is performed in an "inertial" frame defined by the mean equator and equinox at some specified date (reference epoch) and the atomic time scale (TAI). Perturbations are computed in "convenience" frames, which will be explained later, and then rotated into this frame in order to evaluate the equations of motion and the variational equations of state.

The position of the observing stations is defined in a geocentric earth-fixed system which is materialized by a mean pole (e.g., CIO) and a mean Greenwich meridian (e.g., BIH). The observations are tagged with UTC epochs. The link between this system and the inertial system is provided by the Greenwich hour angle of the true vernal equinox and the coordinates of the true celestial pole with respect to the mean pole used. The link between the inertial frame for the integration of the orbit and the true of date frame at the observational epochs is provided by the precession and nutation theories of Newcomb [ESAENA, 1974] and Wahr [1979] respectively. The time scales involved, UT1 and UTC are related to each other using the difference Δ(UT1 - UTC) as obtained from JPL [Fliegel, 1981].

2.313 Gravitational Perturbations

The perturbations due to the Earth's gravitational field were discussed in the previous report. Although that presentation is basically valid,

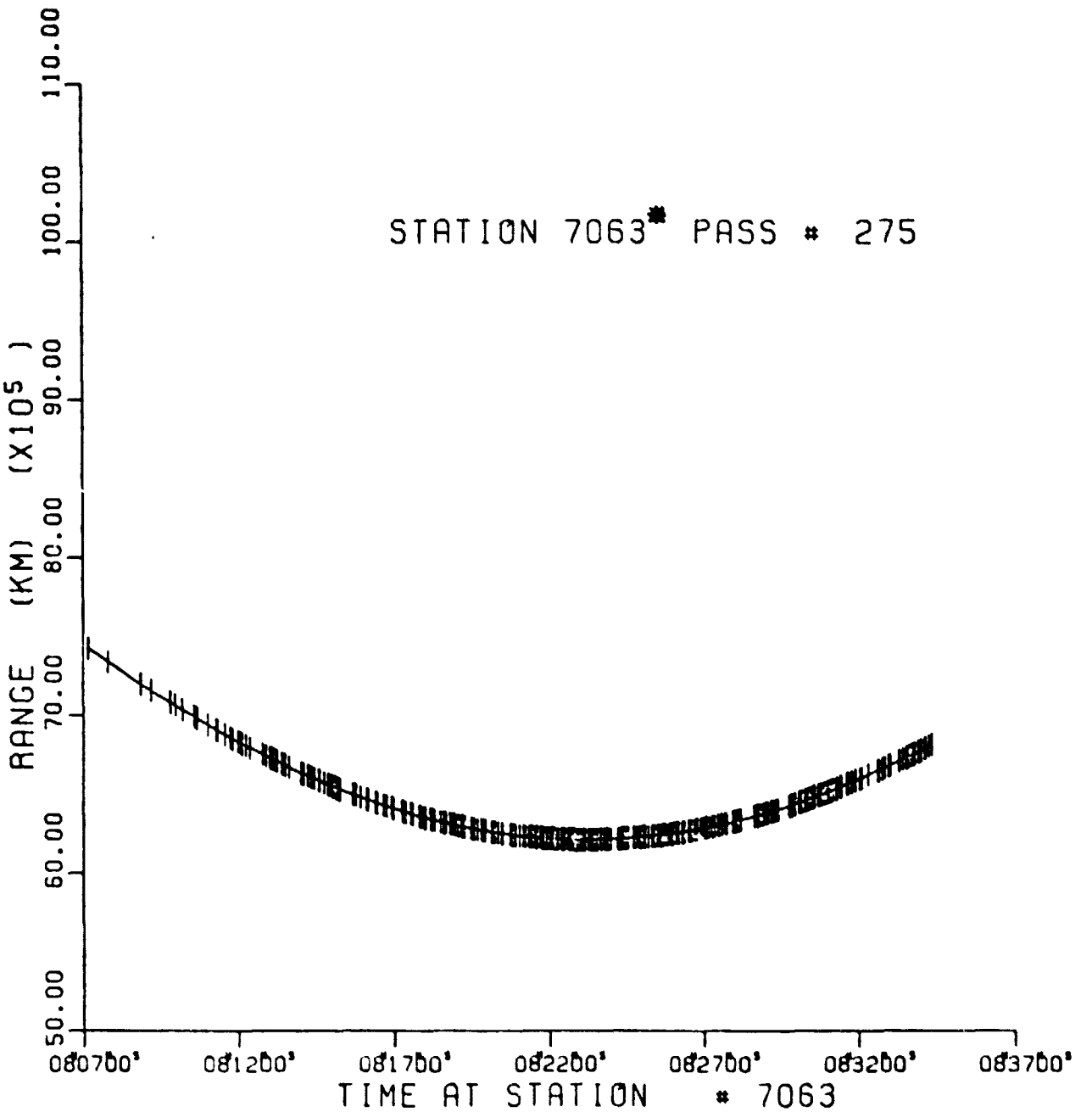
STATION 7063* PASS # 275
RANGE (KM) (X10^5)
110.00
100.00
90.00
80.00
70.00
60.00
50.00
080700'
081200'
081700'
082200'
082700'
083200'
083700'
TIME AT STATION # 7063

Fig. 9a

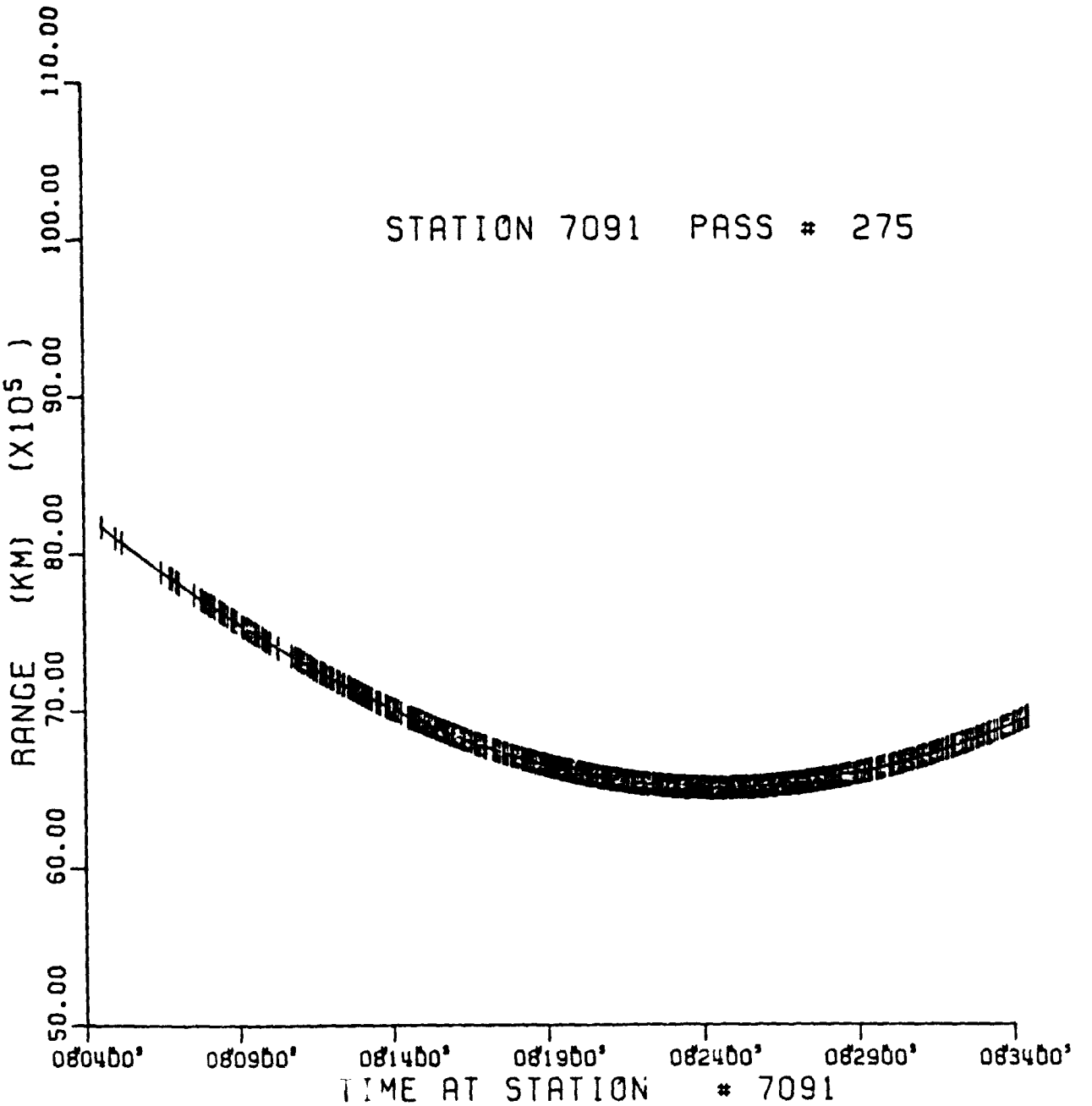
STATION 7091 PASS # 275
RANGE (KM) (X10^5)
110.00
100.00
90.00
80.00
70.00
60.00
50.00
08'04'00"
08'09'00"
08'14'00"
08'19'00"
08'24'00"
08'29'00"
08'34'00"
TIME AT STATION # 7091

Fig. 9b

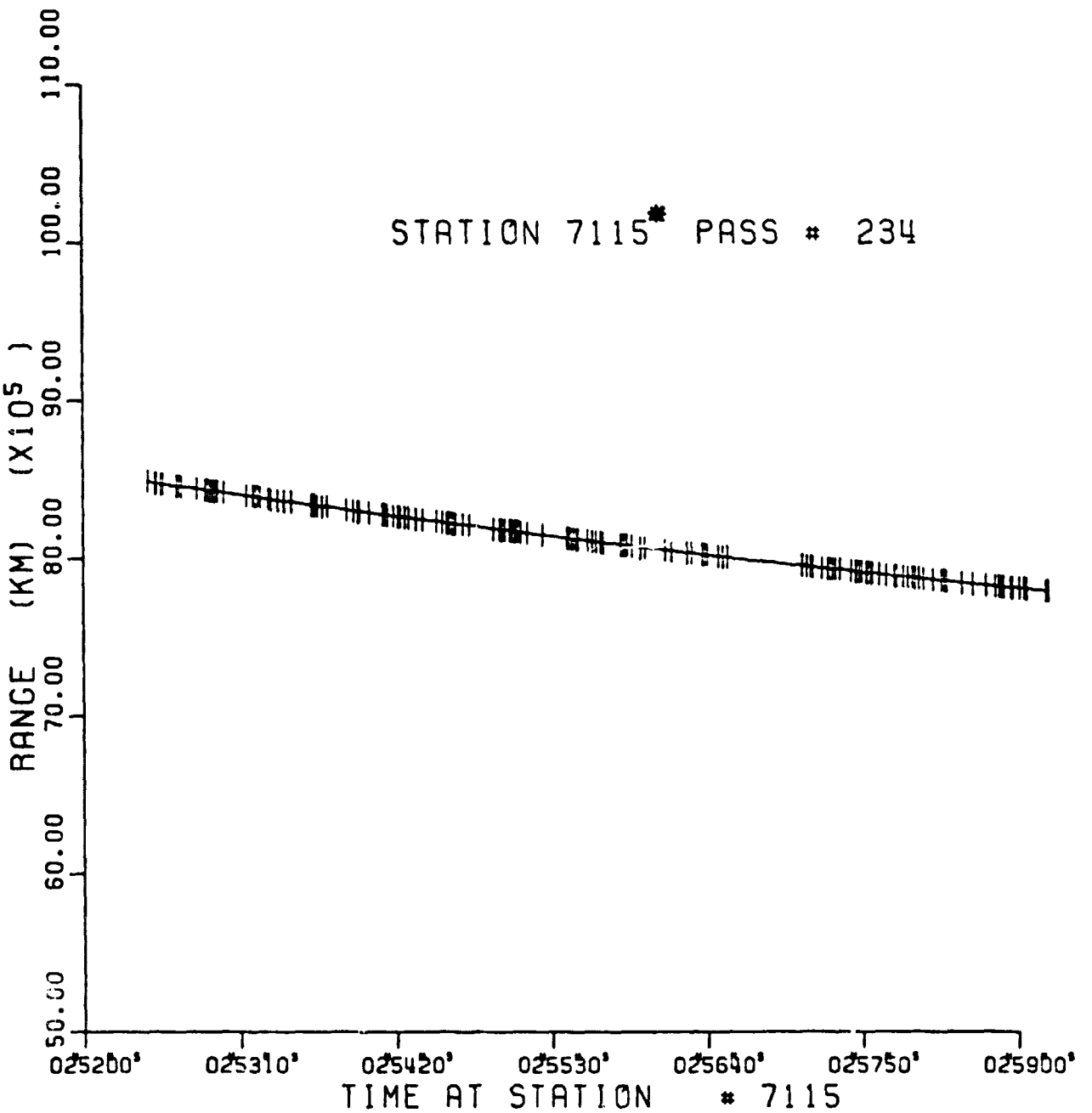
STATION 7115* PASS # 234
RANGE (KM) (X10^5)
110.00
100.00
90.00
80.00
70.00
60.00
50.00
025200'
025310'
025420'
025530'
025640'
025750'
025900'
TIME AT STATION # 7115

Fig. 10a

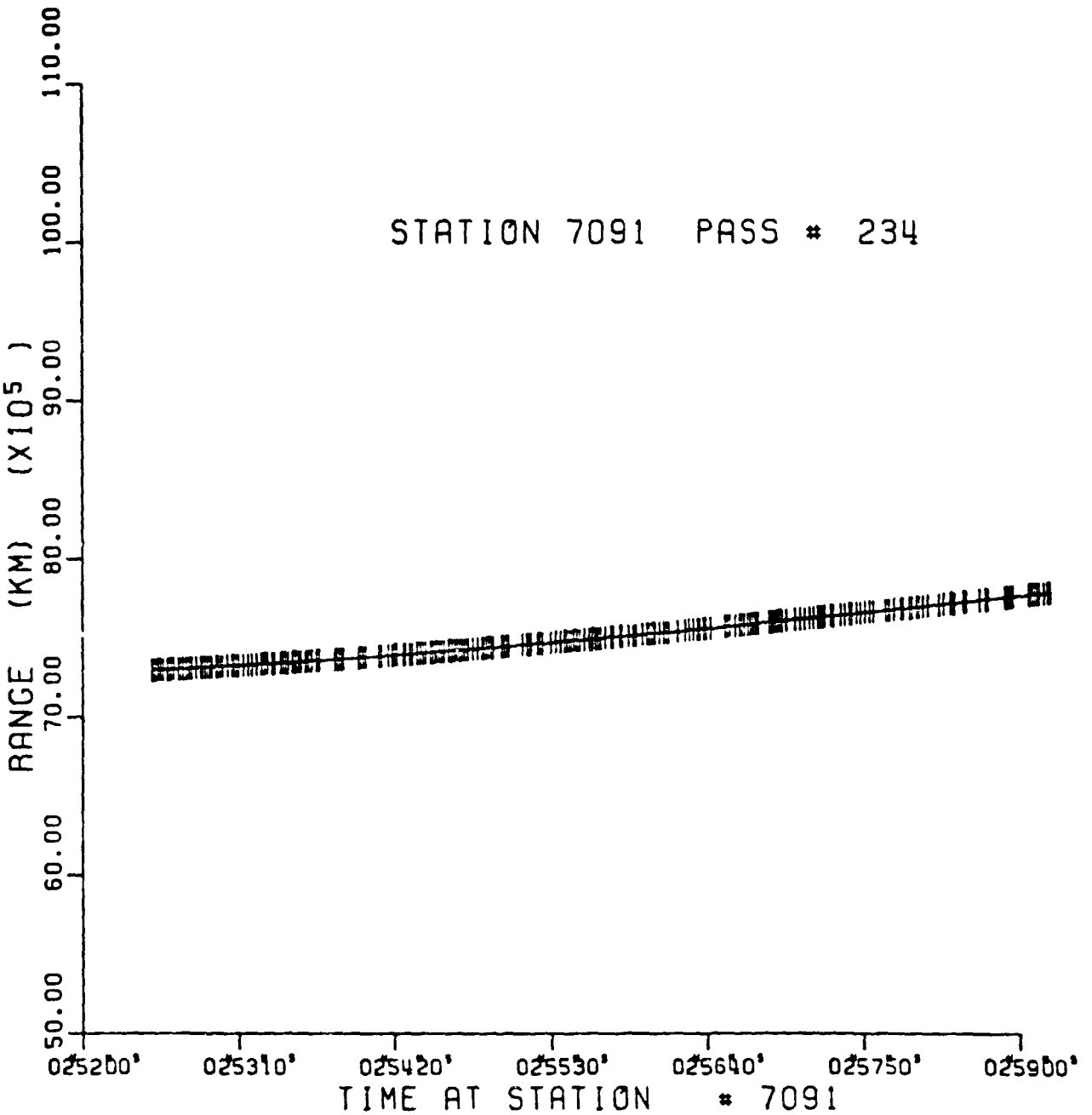
STATION 7091 PASS # 234
RANGE (KM) (X10^5)
110.00
100.00
90.00
80.00
70.00
60.00
50.00
025200'
025310'
025420'
025530'
025640'
025750'
025900'
TIME AT STATION # 7091

Fig. 10b

there is a subtle point in the coordinate system transformations involved which deserves further explanation, especially in view of the existing confusion in the geodetic community. This will be dealt with in the next section. The new version of the program includes point mass accelerations due to the attraction of the moon, the sun, and the planets Venus, Mars, Jupiter and Saturn specified at option by the user. The planetary ephemeris, as well as the lunar and solar position vectors, are obtained by interpolation from the JPL tape containing the DE96 Solar, Lunar and Planetary Ephemeris.

2.314 Computation of the Non-Spherical Effects from the Terrestrial Gravitation

The gravitational potential is usually expressed as a series expansion in spherical harmonics. With the 0^{th}-order term (point mass effect) removed, we can write the non-spherical part of it as:

$$V(r,\phi,\lambda) = \frac{GM}{r}\sum_{n=2}^{\infty}\sum_{m=0}^{n}\left(\frac{a_e}{r}\right)^n [S_{nm}\sin m\lambda + C_{nm}\cos m\lambda]\, P_{nm}(\sin\phi) \qquad (1)$$

where r,ϕ,λ are the spherical coordinates of the point of evaluation. From the purely mathematical point of view the choice or definition of the (r,ϕ,λ) system is irrelevant. The function V, the potential, which is approximated by the series is invariant with respect to any similarity transformation of the underlying coordinate system; the value of V at $P(r,\phi,\lambda)$, V_p will be the same whether P is defined in the (r,ϕ,λ) system or, say, the (r',ϕ',λ') system. The series, however, in (r',ϕ',λ') will have different constants, harmonics, in this case. It is thus obvious that the similarity transformation between (r,ϕ,λ) and (r',ϕ',λ') propagates as a similarity transformation between (C_{nm}, S_{nm}) and (C'_{nm}, S'_{nm}).

So far, the above is just a restatement of already known facts. For instance, Kleusberg [1980] has developed the (rather cumbersome) formulae to obtain the primed harmonics from the original, given the transformation parameters. It is the last statement in the previous paragraph that causes the problems: The fact that a change in the coefficients cannot be attributed to an actual change of the coefficient or a coordinate system change, unless

it is known a priori which of the two happened. In a sense this is similar to "the principle of equivalence" in general relativity, whereby gravitational and inertial forces are inseparable. Considering now that in a dynamical solution the coordinate system definition is provided by the satellite dynamics (short of a longitude definition), one realizes how important it is to clearly define a priori the system in which the harmonics of the series in (1) are referenced. From the geodetic point of view the determination of these harmonics, which is accompanied by a determination of station positions for a large number of globally distributed stations, provides by itself a definition of the underlying coordinate system via the coordinates of these stations. When using such a set of harmonics in a different problem, (e.g., in a partial solution for new station locations), we have two options as to maintaining the internal consistency of the solution: (a) either include observations from the fundamental stations which are constrained to the original positions (very impractical if not impossible), or (b) know a priori the relation of the reference frame for the geopotential to any other frame involved in the solution. The second option, which is practically the only one available to us, will be examined in the following, in connection with the evaluation of the equations of motion and the variational equations of state.

Since the geopotential is given in an earth-fixed system $(r,\phi,\lambda)_b$, it is simpler to compute the required derivatives in that system and rotate the results into the inertial frame of integration:

$$\ddot{\bar{R}}^{I}_{NS} = (SNP)^T M \, \mathbf{V}_b = [P^T N^T S^T M] \mathbf{V}_b \qquad (2)$$

where $\ddot{\bar{R}}^{I}_{NS}$ inertial acceleration due to non-spherical effects

$\mathbf{V}_b = \nabla V(r,\phi,\lambda)$, body-fixed gradient of the potential in $(r,\phi,\lambda)_b$

M the Jacobian which rotates from (r,ϕ,λ) to the (x,y,z) system

S earth orientation rotation for GAST, x_p, y_p

N nutation matrix for the celestial pole

P precession matrix for the celestial pole

The N and P rotations are straightforward and need not concern us anymore.

The matrix S rotates the true of date system into the mean earth-fixed system $(x,y,z)_b$ in which x_p and y_p denote the polar coordinates of the former. The transpose simply reverses the sense of the transformation. This then implies that the vector $M \mathbf{V}_b$ is in the mean earth-fixed system $(x,y,z)_b$, which in turn implies that the matrix M rotates into $(x,y,z)_b$, a vector defined in the $(r,\phi,\lambda)_b$ system, consistent with the expansion of V in (1). If this system happens to be the mean earth-fixed system, then M takes the usual form:

$$M = \begin{bmatrix} \frac{-xz}{r^2\sqrt{x^2+y^2}} & \frac{-y}{x^2+y^2} & \frac{x}{r} \\ \frac{-yz}{r^2\sqrt{x^2+y^2}} & \frac{x}{x^2+y^2} & \frac{y}{r} \\ \frac{\sqrt{x^2+y^2}}{r^2} & 0 & \frac{z}{r} \end{bmatrix} \tag{3}$$

where (x,y,z) are the mean earth-fixed coordinates of the evaluation point. If on the other hand the spherical harmonic expansion in (1) is defined in a system (r',ϕ',λ'), then

$$\mathbf{V}_b = M' \mathbf{V}'_b \tag{4}$$

which implies the following:

(a) The potential gradient $\mathbf{V}'_b$ (r',ϕ',λ') will have to be evaluated using the satellite spherical coordinates in $(r',\phi',\lambda')_b$ rather than $(r,\phi,\lambda)_b$.

(b) In order to use (2), $\mathbf{V}'_b$ will have to be rotated as in (4), to become consistent with the rest of the rotations.

In the general case, therefore, where one accepts that the geopotential refers to a system (r',ϕ',λ'), other than the one implied by the elements of the S matrix, equation (2) must be rewritten as follows:

$$\ddot{\bar{R}}^{I}_{NS} = [P^T N^T S^T M M'] \mathbf{V}'_b \tag{5}$$

where M' is the Jacobian between (r,ϕ,λ) and (r',ϕ',λ')

$\mathbf{V}'_b$ is the gradient of V in (r',ϕ',λ')

and the other matrices are as in (2)

This problem of inconsistency becomes particularly important in the case when one estimates polar motion and earth rotation and then compares

these results to those obtained by other agencies. Even if the same data were used for all solutions, the use of different geopotentials without use of equation (5) will result in systematic differences in the results.

The above comments apply in the same way in the computation of the non-spherical effects contributions in the variational equations:

$$\left[\frac{\partial \dot{\bar{R}}}{\partial \bar{R}}\right]^{I}_{NS} = (SNP)^{T} \left[\frac{\partial \dot{\bar{r}}_b}{\partial \bar{r}_b}\right]_{NS} \left[\frac{\partial r_b}{\partial \bar{R}}\right] \tag{6}$$

Since

$$\bar{r}_b = (SNP)\,\bar{R} \Rightarrow \left[\frac{\partial \bar{r}_b}{\partial \bar{R}}\right] = (SNP) \tag{7}$$

In the computation of $\left[\frac{\partial \dot{\bar{r}}_b}{\partial \bar{r}_b}\right]_{NS}$, the following terms will have to be computed:

$$\left[\frac{\partial r}{\partial \bar{r}_b}\right], \left[\frac{\partial \phi}{\partial \bar{r}_b}\right] \text{ and } \left[\frac{\partial \lambda}{\partial \bar{r}_b}\right] \tag{8}$$

where r,ϕ,λ are the coordinates' arguments of the geopotential V. If these are not consistent with the (x,y,z) system in which $\bar{r}_b$ is referenced, but rather with (x',y',z') such that

$$(x',y',z') = L(x,y,z) \tag{9}$$

then the terms in (8) must be replaced by

$$\left[\frac{\partial r}{\partial \bar{r}_b}\right] = \left[\frac{\partial r}{\partial \bar{r}'_b}\right]\left[\frac{\partial \bar{r}'_b}{\partial \bar{r}_b}\right] = \left[\frac{\partial r}{\partial \bar{r}'_b}\right] L$$

and similarly (10)

$$\left[\frac{\partial \phi}{\partial \bar{r}_b}\right] = \left[\frac{\partial \phi}{\partial \bar{r}'_b}\right] L \quad ; \quad \left[\frac{\partial \lambda}{\partial \bar{r}_b}\right] = \left[\frac{\partial \lambda}{\partial \bar{r}'_b}\right] L$$

In a more compact form, since

$$\left[\frac{\partial \dot{\bar{r}}_b}{\partial \bar{r}_b}\right]_{NS} = \left[\frac{\partial (r,\phi,\lambda)}{\partial \bar{r}_b}\right]^{T} \left[\frac{\partial^2 V}{\partial (r,\phi,\lambda)^2}\right] \left[\frac{\partial (r,\phi,\lambda)}{\partial \bar{r}_b}\right] \tag{11}$$

using (9) and (10), we can write (11) in the most general form as

$$\left[\frac{\partial \dot{\bar{r}}_b}{\partial \bar{r}_b}\right]_{NS} = L^T \left[\frac{\partial(r,\phi,\lambda)}{\partial \bar{r}_b'}\right]^T \left[\frac{\partial^2 V}{\partial(r,\phi,\lambda)^2}\right] \left[\frac{\partial(r,\phi,\lambda)}{\partial \bar{r}_b'}\right] L \qquad (12)$$

and denoting by

$$Q = \left[\frac{\partial(r,\phi,\lambda)}{\partial \bar{r}_b'}\right]$$

equation (6) becomes in the general case

$$\left[\frac{\partial \dot{\bar{R}}}{\partial \bar{R}}\right]^I_{NS} = (SNP)^T L^T Q^T \left[\frac{\partial^2 V}{\partial(r,\phi,\lambda)^2}\right] Q L (SNP) \qquad (13)$$

or

$$\left[\frac{\partial \dot{\bar{R}}}{\partial \bar{R}}\right]^I_{NS} = [Q L S N P]^T \left[\frac{\partial^2 V}{\partial(r,\phi,\lambda)^2}\right] [Q L S N P] \qquad (14)$$

This discussion would hardly be complete if one did not identify where the real problem lies: Why geopotential models obtained from similar types and amounts of data differ in the coordinate system definition. The obvious reason would be that the stations which participate in the observations and define (with their estimated coordinates) the reference frame in each case are different. This is true, but in practice it is a large number of globally distributed stations which participate in such campaigns and one would think that on the average the geometry would have little effect, certainly not introducing biases with respect to certain regional sub-networks. The problem seems to lie in the neglect of certain physical phenomena, affecting the harmonics themselves, in the process of their estimation. It is a well known fact [Heiskanen and Moritz, 1967; Nagel, 1976] that for the low-degree harmonics (up to n=2) we can easily associate with them certain properties of the estimated model. The pair (C_{21}, S_{21}) is of particular interest to us since their values are directly proportional to the alignment of the reference system with the principal axis of maximum moment of inertia. Lambeck first called attention to the implications of this otherwise innocent looking property, in [Lambeck, 1971], where he stated that

$$u^* = \frac{C_{21}}{C_{20}} \qquad \text{and} \qquad v^* = -\frac{S_{21}}{C_{20}} \tag{15}$$

u^* and v^* being the coordinates of the axis of figure with respect to the third axis of the reference coordinate system (the axes u^*,v^* are defined in the same sense as the x_p,x_p for the pole). A proof for (15) can be found in [Nagel, 1976]. This interesting property becomes a real problem in practice, due to the fact that the axis of figure is time variant. In [McClure, 1973; Nagel, 1976; Leick, 1978; and Moritz, 1979], one will find detailed descriptions of the motions of this axis. It suffices here to mention that there is a free motion with an amplitude of 2m and a period equal to that of the Chandlerian wobble ($\sim$ 430 days) and a forced diurnal motion with an amplitude equal to 60 m! The elastic-earth-model motions for the various axes involved are depicted in Fig. 11, taken from [Nagel, 1976]. Figs. 12 and 13 [Nagel, 1976] show the diurnal variation of C_{21} and S_{21} due to the diurnal motion of the axis of figure. In Fig. 14 [ibid.], the diurnal variations have been filtered out and the effects of the free motion on C_{21} and S_{21} are shown, based on the BIH polar motion over 1968.0 - 1973.0 period (from which the motion of the axis of figure has been deduced). It is obvious from these graphs that if one is trying to clearly define the coordinate system to which the estimated harmonics refer, one cannot afford to neglect such effects. Since the observations used in such major solutions span quite a long period of time (over five years in most cases), it is quite impossible to keep the coordinate system definition intact while at the same time solving only for average values of C_{21} and S_{21}. As it was shown in this discussion, an improper coordinate system transformation in a later solution will introduce biases in the orbit and in the estimated parameters based on that orbit (e.g., polar motion). Based on the above, it seems that the only procedure which will produce confusion-free results is the one in which the timelike variations of C_{21} and S_{21} have been considered in the determination of the geopotential harmonics and the solution is performed for a prespecified epoch. In this sense, the orientation of the coordinate system in which the geopotential is referenced will be determined by the adopted model for the axis of figure motion, while the geocentricity of the system will still be maintained by the suppression of the first-degree harmonics. The motions of the axis of figure do not affect only

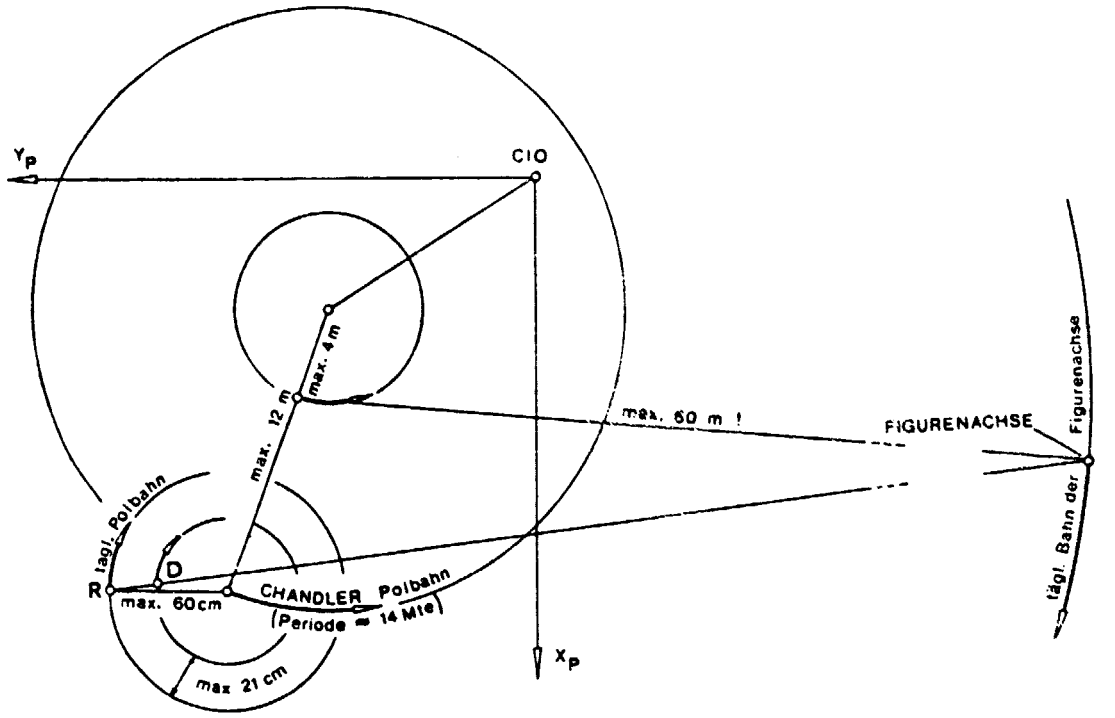
Y_P
CIO
max. 4 m
max. 12 m
max. 60 m !
FIGURENACHSE
Figurenachse
tägl. Bahn der
tägl. Polbahn
D
R
max. 60cm
CHANDLER Polbahn
(Periode ≈ 14 Mte)
max 21 cm
X_P

Fig. 11

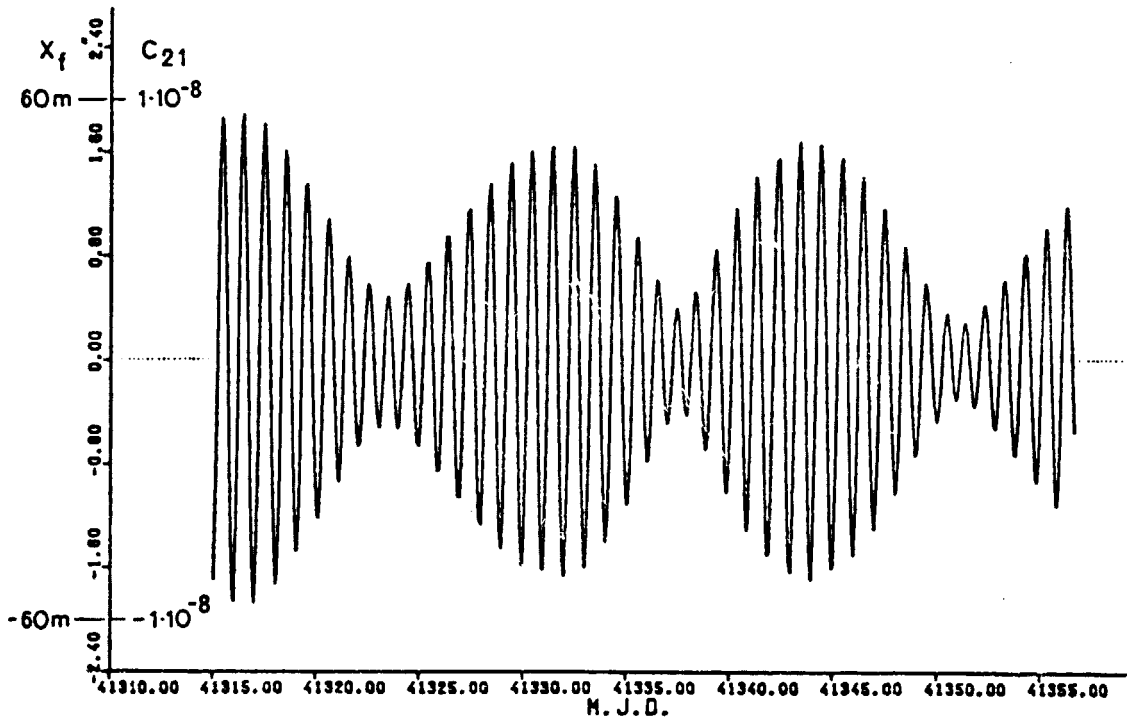
X_f
C21
60m
1·10^-8
-60m
-1·10^-8
2.40
1.60
0.80
0.00
-0.80
-1.60
-2.40
41310.00
41315.00
41320.00
41325.00
41330.00
41335.00
41340.00
41345.00
41350.00
41355.00
M.J.D.

Fig. 12

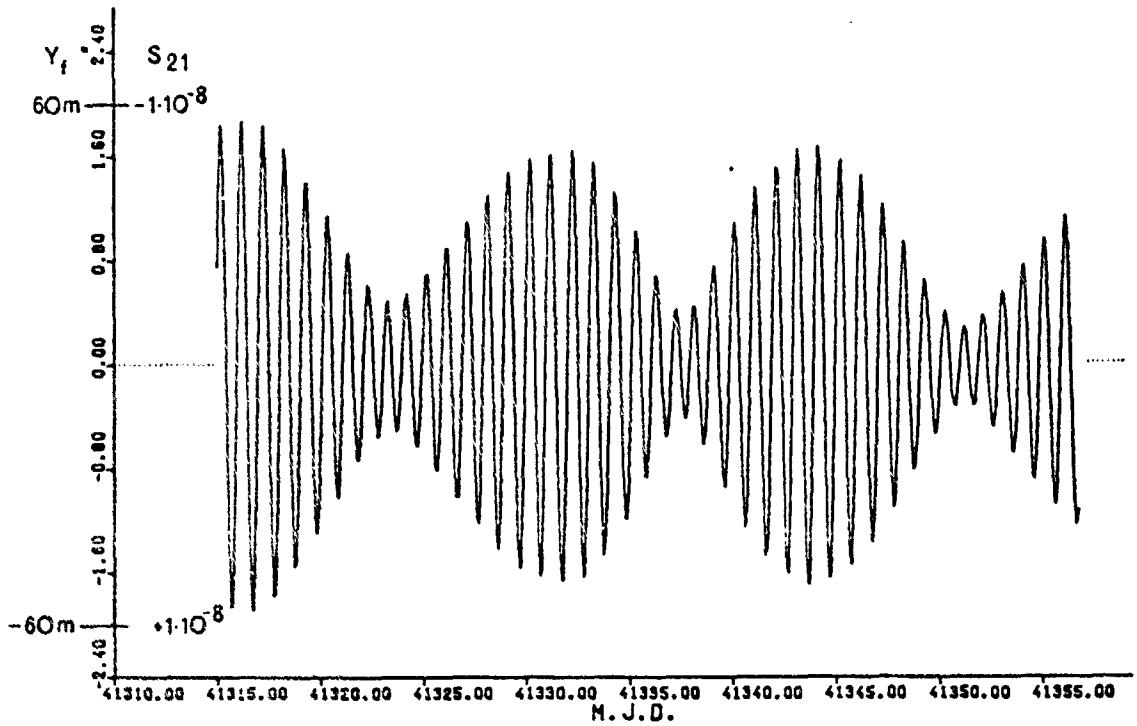
Y_f
S21
60m
-1·10^-8
+1·10^-8
-60m
2.40
1.60
0.80
0.00
-0.80
-1.60
-2.40
41310.00
41315.00
41320.00
41325.00
41330.00
41335.00
41340.00
41345.00
41350.00
41355.00
M.J.D.

Fig. 13

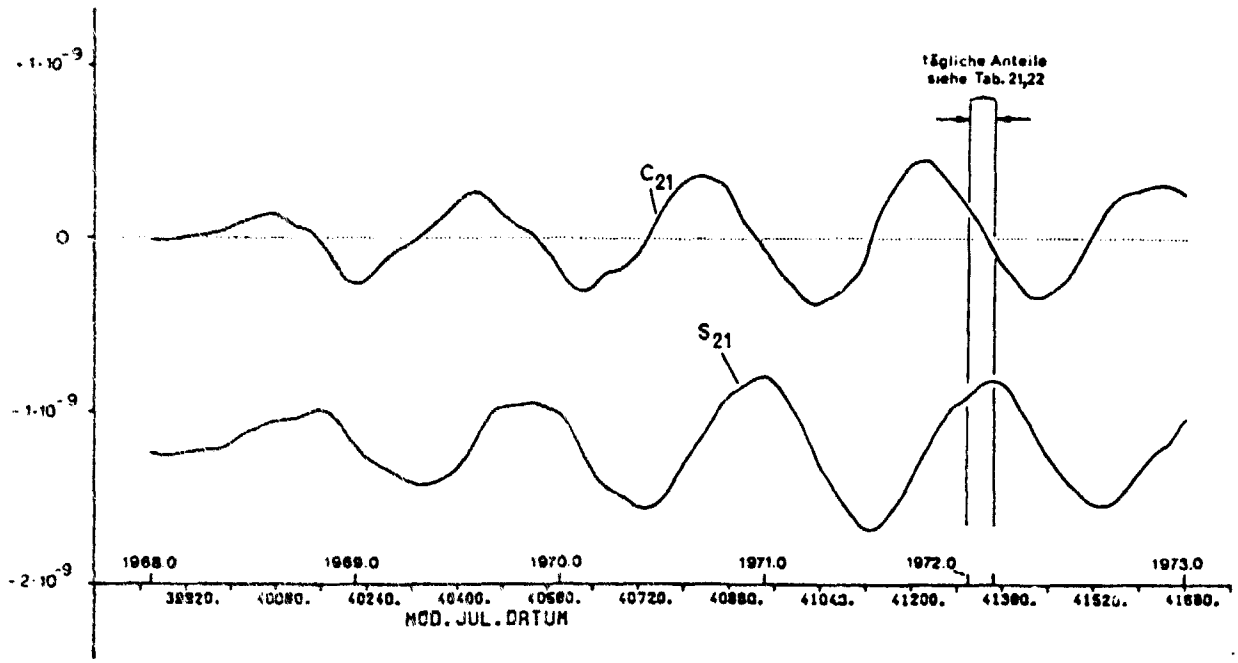
+1·10^-9
0
-1·10^-9
-2·10^-9
tägliche Anteile
siehe Tab. 21,22
C21
S21
1968.0
1969.0
1970.0
1971.0
1972.0
1973.0
39920.
40080.
40240.
40400.
40560.
40720.
40880.
41043.
41200.
41360.
41520.
41680.
MOD. JUL. DATUM

Fig. 14

C_{21} and S_{21}, but the effects on the rest of the harmonics are well below the order of 10^{-14}, and for the time being they can be safely neglected.

2.315 Perturbations from the Solid Earth Tides

The model for the tidal potential is a rather simplified one accounting for effects to degree n=2 only:

$$U_{T_2} = \frac{GM_b}{R_b^3} R_e^2 P_2(\cos\phi) \tag{16}$$

Assuming that for an elastic earth $k_2 \simeq 0.29$, the disturbing potential due to a body b at a satellite position $\bar{r}$ will be:

$$U_D(r) = \frac{k_2}{2} \frac{GM_b}{R_b^3} \frac{R_e^5}{r^3} [3(\bar{u}_b \cdot \bar{u}_r)^2 - 1] \tag{17}$$

where $\bar{u}_b$ and $\bar{u}_r$ denote unit vectors in the directions of the disturbing body and the satellite respectively. The acceleration sensed by the satellite is $\ddot{\bar{R}}_T = \nabla U_D(r)$, or from (17):

$$\ddot{\bar{R}}_T = -\frac{3}{2} k_2 \left(\frac{GM_e}{R_e^2}\right)\left(\frac{M_b}{M_e}\right)\left(\frac{R_e}{R_b}\right)^3 \left(\frac{R_e}{r}\right)^4 \left([1 - 5(\bar{u}_b \cdot \bar{u}_r)^2]\, \bar{u}_r + 2(\bar{u}_b \cdot \bar{u}_r)\, \bar{u}_b\right) \tag{18}$$

The contribution in the variational equations is the following:

Let: $C = -\frac{3}{2} k_2 \frac{GM_e}{R_e^3}\left(\frac{M_b}{M_e}\right)\left(\frac{R_e}{R_b}\right)^3\left(\frac{R_e}{r}\right)^5$

then:

$$\left[\frac{\partial \ddot{\bar{R}}_T}{\partial \bar{r}}\right] = C\left\{[3(\bar{u}_b \cdot \bar{u}_r)^2 - 5]\, \bar{u}_r\, \bar{u}_r^T + 2\bar{u}_b\, \bar{u}_b^T + [1 - 5(\bar{u}_b \cdot \bar{u}_r)^2]\, I - 10(\bar{u}_b \cdot \bar{u}_r)[\bar{u}_r\, \bar{u}_b^T + \bar{u}_b\, \bar{u}_r^T]\right\} \tag{19}$$

and

$$\left[\frac{\partial \ddot{\bar{r}}_T}{\partial \dot{\bar{r}}}\right] = [\phi_3]$$

The above formulae must be summed over the bodies contributing in the tides. In GEOSPP81, the lunar and solar effects are the only ones considered.

2.316 Solar Radiation Pressure Perturbations

The model implemented in the program is a rather simple one, considering only mean solar flux effects. The acceleration is given as

$$\ddot{\bar{R}}_{SR} = \nu \frac{S}{c} R_{SUN}^2 \frac{C_R A}{m} \frac{\bar{R}_{vs}}{|\bar{R}_{vs}|^3} \; ; \quad \bar{R}_{vs} = \bar{r} - \bar{R}_s \tag{20}$$

where

ν = shadow factor = 1- sunlight, or 0- shadow
S = mean solar flux at 1 AU
c = speed of light in vacuum
C_R = radiation reflectivity coefficient for the satellite
A = cross-sectional area perpendicular to direction of incidence
m = satellite mass
R_{SUN} = mean distance of earth-sun centers of mass (= 1 AU)
$\bar{r}$ = satellite position vector
$\bar{R}_s$ = sun's position vector

From simple geometric considerations

$$\nu = 1 \text{ if } \bar{r}\cdot\bar{R}_s > 0, \text{ or if } \bar{r}\cdot\bar{R}_s < 0 \text{ but } \left| \bar{r} - \frac{(\bar{r}\cdot\bar{R}_s)}{|\bar{r}|\,|\bar{R}_s|} \bar{R}_s \right| > R_e$$

From (20) the contribution to the variational equations is obtained as

$$\left[\frac{\partial \ddot{\bar{R}}_{SR}}{\partial \bar{r}}\right] = \nu \frac{S}{c} R_{SUN}^2 \frac{C_R}{|\bar{R}_{vs}|^3} \frac{A}{m} \left\{ I - 3 \frac{\bar{R}_{vs}\,\bar{R}_{vs}^T}{|\bar{R}_{vs}|^2} \right\} \tag{21}$$

and

$$\left[\frac{\partial \ddot{\bar{R}}_{SR}}{\partial \dot{\bar{r}}}\right] = [\phi_3]$$

Sections 5 and 6 are explained in detail in [Cappellari et al., 1976].

References

Cappellari, J.O. et al. (1976) "Mathematical Theory of the Goddard Trajectory Determination System," GSFC X-582-76-77, NASA Goddard Space Flight Center, Greenbelt, Maryland.

Explanatory Supplement to AENA (1974) Her Majesty's Stationery Office, London.

Fliegel, H.F. et al. (1981) "Earth Rotation (UTϕ) from Lunar Laser Ranging," 3rd Annual NASA Geodynamics Program Review, JPL, Pasadena, Calif.

Heiskanen, W.A. and H. Moritz (1967) Physical Geodesy, Freeman, San Francisco.

Kleusberg, A. (1980) "The Similarity Transformation of the Gravitational Potential," manuscripta geodaetica 5, 4, pp. 241-256.

Lambeck, K. (1971) "Determination of the Earth's Pole of Rotation from Laser Range Observations to Satellites," Bull. Geodesique, No. 101.

Leick, A. (1978) "The Observability of the Celestial Pole and Its Nutations," Dept. of Geodetic Science Rept. No. 262, Ohio State Univ., Columbus.

McClure, P. (1973) "Diurnal Polar Motion," GSFC X-592-73-259, NASA Goddard Space Flight Center, Greenbelt, Maryland.

Moritz, H. (1979) "Concepts in Geodetic Reference Frames," Dept. of Geodetic Science Rept. No. 294, Ohio State Univ., Columbus.

Nagel, E. (1976) "Die Bezugssysteme der Satellitengeodäsie," Deutsche Geodätische Kommission, Heft 223, Reihe C, Munich.

Wahr, J.M. (1979) "The Tidal Motions of a Rotating, Elliptical, Elastic and Oceanless Earth," PhD dissertation, University of Boulder, Colorado.

2.32 Doppler Experiments

Introduction

The idea of using ranges derived through simultaneous Doppler observations for a geometric solution has been fully explained in the previous semiannual report. It should be useful though to note that the data used for this experiment is the EDOC-2 campaign data set. There has been some progress in a small experiment involving observations from six stations which is the minimum for a geometric solution. However, an effort has just begun to perform the same solution with more stations involved and many more common observations included. Progress and problems arising during this effort will be included in this report.

Additionally, there has been another Doppler experiment which started a few months ago. This is also a geometric range solution, this time using a different set of simultaneously obtained Doppler data. This data set is the Victoriaville data sent to us from the Ministere de l'Energie et des Resources of Canada. At the end of this chapter, progress on this effort will be reported.

2.321 Geometric Solution Using Ranges Derived Through Simultaneous Doppler Observations

The Ranges

The Doppler derived ranges have been evaluated according to the theory described in the previous semiannual report. These ranges which are the observations in our adjustment should be very close to the corresponding geometrically derived ranges. The geometrically derived ranges are those evaluated through the formula

$$r = ((X_G - X_S)^2 + (Y_G - Y_S)^2 + (Z_G - Z_S)^2)^{\frac{1}{2}}$$

where X_G, Y_G, Z_G are the earth-fixed Cartesian coordinates referring to the ground stations. X_S, Y_S, Z_S are the satellite's earth-fixed Cartesian coordinates derived through the broadcast ephemeris.

Indeed, the Doppler derived and the geometrically derived ranges have been compared through graphs and their differences were not really significant especially in that part of the pass where the range decreases (the elevation

angle increases). AFter the satellite reaches the highest elevation angle, the aforementioned difference becomes larger (sometimes 5 km) but still with such differences the geometrically derived ranges can be used as approximate ranges in the adjustment.

The Geometric Range Adjustment

The mathematical model used for the geometric range adjustment is the following:

$$\hat{r} = [(X_S - X_G)^2 + (Y_S - Y_G)^2 + (Z_S - Z_G)^2]^{\frac{1}{2}} + a_o + f(p) \qquad (1)$$

where a_o is a constant bias including the error to the initial range plus the error due to clock offset among the stations; f(p) is a function of any kind of parameters affecting the observations (Doppler ranges). We will call the a_o + f(p) part of the mathematical model the residual model. We will call preliminary adjustment the part of the adjustment where we keep the station coordinates fixed and we solve for the satellite coordinates and the coefficients of the residual model.

The next step was to come up with a residual model which yields convergence and the smallest after-adjustment residuals possible. The method used was the following: First we performed a preliminary adjustment without using any kind of residual model. Our mathematical model was

$$\hat{r} = [(X_S - X_G)^2 + (Y_S - Y_G)^2 + (Z_S - Z_G)^2]^{\frac{1}{2}} \qquad (2)$$

Then we tried to study the behavior of the residuals from this adjustment. These residuals have been plotted and the plots have been compared to each other for all the stations and the passes.

The fact is that the part of the passes used for the adjustment is really small (about 10 minutes) to give a good estimation of the behavior of the residuals, but in all the cases we dealt with they had more or less the following pattern: Relatively small in the beginning, increasing positively or negatively with time, showing a second degree or sometimes a third-degree polynomial behavior. The uncertainty in choosing one residual model led us to try using different models and study the rapidity of convergence and the magnitude as well as the behavior of the new residuals. The residual models tested were the following:

(a) $v = a_o + b_o t$

(b) $v = a_o + b_o t + c_o t^2$

(c) $v = a_o + b_o t + c_o \operatorname{cosec} e$

(d) $v = a_o + b_o t + c_o r$

(e) $v = a_o + b_o t + c_o t^2 + d_o r$

where v are the range residuals derived using the mathematical model described in eq. (2), t is the time of the particular observation, e is the corresponding elevation angle, and r is the range itself corresponding to the particular observation.

From all these models, (b) has been proven to yeild the smallest post-preliminary adjustment residuals as well as to be the fastest converging model. The linear model (a) yields post-preliminary adjustment residuals fairly large (to the order of 100 m) and having sinusoidal behavior. The residual model (c) yields an oscillating solution in terms of determining the position of the satellite as well as in determining a_o, b_o, and c_o residual model coefficients.

Finally, using models (d) and (e) we did not have convergence in our preliminary adjustment. Therefore, the mathematical model we decided to adopt is the following:

$$\dot{r} = [(X_S - X_G)^2 + (Y_S - Y_G)^2 + (Z_S - Z_G)^2]^{\frac{1}{2}} + a_o + b_o t + c_o t^2$$

The post-preliminary adjustment residuals we get using this model are of the order of 0.5 - 1 m during the biggest part of the pass, but they systematically become large (about 10 m) towards the end of the pass. Presently we are trying to explain somehow the systematic behaviorwhich has not been eliminated using all the previously mentioned residual models.

It has been mentioned in the previous semiannual report that 19 passes have been selected to be included in the final adjustment. Fig. 15 shows how the projections of these common passes are located with respect to six observing stations. Some of the passes are not close to the observing stations. Their elevation angles are small and in the preliminary adjustment they converge very slowly in terms of satellite coordinates yielding very large residuals. There is one pass for which the common part starts right above station LGA in Spain. For this pass due to loss of information we have no convergence in the preliminary adjustment.

After all these investigations we came up with nine good passes consisting of 5694 common observations totally. This is probably not a good number for a strong geometric solution, but the experiment will be performed with those few observations and depending on the results we get we will add more passes in the future.

60°
55°
50°
45°
40°
35°
30°
25°
20°
30°
25°
20°
15°
10°
5°
0°
-5°
-10°
-15°
-20°
-25°
+GBR
+CBRP
+VLF
+DNS
1
2
3
4
5
6
7
8
9
10
11
12
13
14
15
16
17
18
19

Fig. 15

2.322 The Extended Geometric Range Adjustment

A new attempt began a few months ago in the Department of Geodetic Science to perform a geometric range adjustment covering a large area in Europe. The data set used for this purpose is also the EDOC-2 campaign data set. Performing such a large geometric range adjustment we will be able to compare the results derived from various dynamic solutions performed by several European agencies. For this purpose all the stations equipped with JMR and CMA receivers from which data is available, 23 stations totally, have been selected initially to participate in this experiment.

The Data Editing

The first step in data editing was to write a program which takes as input all the tapes as sent from Europe and performs the following operations:

1. Identifies the passes
2. Rejects bad observations. This has as a result the break of the pass into two or more parts. We characterize as bad observations:
   a) those which have a recorded time interval which is not 4.6 or 4.9 s
   b) every 25th observation which does not have a 4.9 s time interval
   c) every 26th observation which does not start with an even 2 minute mark
   d) observations for which the recorded Doppler counts are not within the possible limits

The output of this program is the information for each observation needed for the computation of ranges. The output also includes information for each individual pass containing the meteorological data for the tropospheric refraction.

The next step was to find the common observations. For this purpose, a new program has been written which gives the parts of the passes which have been simultaneously observed from at least six stations. Using this program we came up with more than 400 common passes with length varying between 2 and 10 minutes. All the passes have also been plotted with respect to time and station and from this diagram it is very easy to identify their common parts.

This experiment will continue in the same pattern as the small one including the six stations in Spain, and we hope it will give a complete image of the advantages and the disadvantages of the new method of simultaneous Doppler ranging.

2.323 The Victoriaville Data Set

The last experiment involving a geometric range solution is one performed with the Victoriaville data set including Doppler observations from eight stations. These observations took place between October 2-4, 1979. These data have been used by Sheltech, Ltd. under contract with Quebec Lands and Forests for the purpose of evaluating the accuracy of Doppler survey methods for establishing network control. The participating stations' locations are given in the following table:

	ϕ	λ	h
1	45°45'26".0040	72°16'38".1797	218.29 m
2	45 37.6413	11 39.2460	172.60
3	52 16.2391	15 43.2894	104.02
4	57 55.3552	02 58.1076	158.33
5	55 34.8419	07 52.7973	112.82
6	56 53.5586	16 09.4327	101.60
7	51 01.6013	04 59.7844	132.27
8	49 52.5628	00 58.5315	124.22

The observed satellites were 30190, 30140, 30130, 30120 and 30200.

The Victoriaville data have been sent to us on one tape including the Doppler counts, timing information, broadcast ephemeris information and signal strength information. All these data were already majority voted.

From the broadcast ephemeris information of the tape, using H. White's program, the observed satellites' state vectors have been derived. For two of the observed satellites, specifically 30140 and 30190, the precise ephemeris was available and therefore a comparison of the state vectors was possible. The state vectors for these two satellites were very close which fact assured us of the efficiency of H. White's program. Meteorological data for this data set has been sent separately. These meteorological data have been recorded at the locations of the stations every ten minutes and include temperature, relative humidity and barometric pressure.

The data as they have been sent to us have been used as input in the program JMR DOP-A provided by NGS and have been transformed to a format useful for further processing.

2.324 Doppler Intercomparison Experiment

Work is still continuing on the programs which will be used to reduce the data from the OSU Doppler Intercomparison Experiment (which was described in the Fourth Semiannual Report). Serious problems were encountered which prevented the use of the CALSAGA program for the final data reduction. Therefore the program system GEODOP has been obtained from the Canadian Geodetic Survey for this purpose. Work is underway to convert this CDC Fortran program to IBM Fortran for use on our system and to allow input of our intercomparison data.

Problems with GALSAGA

As explained in the last semiannual report, the GALSAGA (or SAGA) and SAMVAP [Brown, 1973] programs and the preprocessing programs written here (SUPASS and SAGSET) were to have been used to process the intercomparison data. However, after numerous test runs with some JMR-1A data, it was apparent that the GALSAGA program would not converge to a reasonable solution. These test runs included the use of: a) up to 40 balanced satellite passes, b) various program constraints; c) direct and SAMVAP created precise ephemeris state vectors to establish the orbit, d) various weights for the station, state vector, and program constraints.

The best solutions obtained during these tests resulted in final station positions which were incorrect by several hundred meters, unreasonable values for orbital and other parameters, and values for V^TPV of the adjustment which were far too high, even after up to ten iterations of the solution. There seem to be two possible explanations for these poor solutions. The first is based on the observation that GALSAGA was intended to be used for range observations, even though it does contain input provisions for Geoceiver data. It is slightly possible that some error had been made in the programming here to allow it to use JMR (and other) data, although this is not likely since it has been used successfully here for multi-stations solutions of JMR data [Arur, 1977], with only slight modification

since then. The second explanation is far more likely, being that GALSAGA will only operate well for multi-station solutions, since it is after all a short-arc program. A single station solution might not converge unless all coordinates (station and satellite) and parameters are very highly constrained. The fact that there appears to be no specific references to single station GALSAGA solutions supports this conclusion.

However, some further use of the GALSAGA program is still being considered. It is possible that another attempt at a single station solution may be made (with different data). If a single station solution can be obtained GALSAGA solutions could then be compared with GEODOP solution. More importantly, GALSAGA may be used to process multi-station solutions for the Columbus-Ottawa baseline for which we have data. (There presently is no reason to suspect that the OSU version of GALSAGA will not work with two or more station solutions.) Therefore some work is being done to modify the SUPASS and SAGSET programs to:

a) Read majority voted data in a PREDOP compatible format, to allow solutions with either GALSAGA or GEODOP with the same data sets,

b) Use "30 second" Doppler counts instead of "4.6 second" counts, again to maintain compatibility with GEODOP and to reduce the computational expense in running GALSAGA,

c) allow SAGSET to input multi-station solutions to GALSAGA. It should be noted, however, that this work will be of low priority, especially if our GEODOP version will allow us to adequately answer the original problems (as posed in the Fourth Semiannual Report.

GEODOP Program Sytem

Since solutions could not be obtained with the GALSAGA program, Mr. Jan Kouba of the Canadian Geodetic Survey (CGS) was contacted to determine the availability of his GEODOP program and assoicated subprograms (such as PREDOP, PREPAR, MERGE, NWLFIT, etc.), herein called the GEODOP program system [Kouba, 1976]. Through Mr. Kouba, the CGS provided us with a tape copy of the latest versions of the programs in CDC Fortran, along with the program manuals and updates to them. Since it would be necessary to fully understand the programs' operation, and to convert them to IBM Fortran, Brent Archinal of OSU traveled to Ottawa to confer with Mr. Kouba and others about the program system and to run some of the OSU data. These computer runs would then be

available for comparison with runs here to check our IBM version of the program.

The conversion to the IBM Fortran is now well underway, with the PREDOP and GEODOP programs now in operating condition here, except for a few problems still being worked on. The program system presently accepts CMA-751 majority voted data, with subroutines available (but still being tested) to use MX-1502 raw data, and JMR-1A majority voted data. In the near future, we expect to: a) Finish the PREDOP and GEODOP conversion, and testing of the input subroutines, b) test our conversions of the other utility programs in the system (MERGE, NWLFIT, etc.), c) Design the JCL language to operate the programs with the large amount of data (files) which will be used.

After these conversions are tested and complete, the Columbus and Columbus-Ottawa Intercomparison data will be processed as explained in the Fourth Semiannual Report, the eventual goal being the determination of the most accurate instrument type. These programs will also probably be used to reduce the OSU Institute of Polar Studies Greenland Doppler data, and possibly to provide checks on the geometric Doppler Solutions now being made here.

References

Arur, M.G. (1977) "Experiments for Improved Positioning by Means of Integrated Doppler Satellite Observations and the NNSS Broadcast Ephemeris," Dept. of Geodetic Science Rept. No. 258, Ohio State Univ., Columbus.

Brown, D.C. and J.E. Trotter (1973) "Extension to SAGA for the Geodetic Reduction of Doppler Operations," DBA Systems Inc., Melbourne Florida.

Kouba, J and J.D. Boal (1976) Program GEODOP, Dept. of Energy, Mines and Resources, Ottawa, Ontario.

3. PERSONNEL

Ivan I. Mueller, Project Supervisor, part time

Brent Archinal, Graduate Research Associate, part time

Yehuda Bock, Graduate Research Associate, part time

George Dedes, Graduate Research Asociate, part time

Carol Feole, Student Clerical Assistant, part time

Erik W. Grafarend, Consultant, without compensation

Despina E. Pavlis, Graduate Research Associate, part time

Erricos C. Pavlis, Graduate Research Associate, part time

Baldev Singh Rajal, Graduate Research Associate, supported by Department of Geodetic Science, part time

Rudi Schneeberger, Graduate Research Associate, supported by Department of Geodetic Science, part time

Irene B. Tesfai, Secretary, part time

Zhu Sheng-Yuan, Visiting Scholar, without compensation

4. TRAVEL

I.I. Mueller and E.C. Pavlis — October 1-2, 1980
Greenbelt, Maryland
To attend third meeting of Lageos Working Group at Goddard Space Flight Center

I.I. Mueller
San Francisco — December 6-10, 1980
To attend Annual Fall Meeting of the American Geophysical Union and present a paper.

Brent Archinal
Ottawa, Canada — December 16-19, 1980
Discussions with Jan Kouba at Earth Physics Branch, Energy, Mines and Resources Canada

E.C. Pavlis, Y. Bock and Y.S. Zhu
Greenbelt, Maryland — January 25-30, 1981
To attend Crustal Dynamics AO Preproposal Conference and 3rd Annual Geodynamics Program Review, presentation made by E.C. Pavlis.

Ivan I. Mueller
Greenbelt, Maryland — January 28-29, 1981
To attend Crustal Dynamics AO Preproposal Conference and 3rd Annual Geodynamics Program Review and make a presentation.
No support from the projects.

5. REPORTS PUBLISHED TO DATE

OSU Department of Geodetic Science Reports published under Grant No. NSG 5265:

262 The Observability of the Celestial Pole and Its Nutations
by Alfred Leick
June, 1978

263 Earth Orientation from Lunar Laser Range-Differencing
by Alfred Leick
June, 1978

284 Estimability and Simple Dynamical Analyses of Range (Range-Rate and Range-Difference) Observations to Artificial Satellites
by Boudewijn H.W. van Gelder
December, 1978

289 Investigations on the Hierarchy of Reference Frames in Geodesy and Geodynamics
by Erik W. Grafarend, Ivan I. Mueller, Haim B. Papo, Burghard Richter
August, 1979

290 Error Analysis for a Spaceborne Laser Ranging System
by Erricos C. Pavlis
September, 1979

298 A VLBI Variance-Covariance Analysis Interactive Computer Program
by Yehuda Bock
May, 1980

299 Geodetic Positioning Using a Global Positioning System of Satellites
by Patrick J. Fell
June, 1980

302 Reference Coordinate Systems for Earth Dynamics: A Preview
by Ivan I. Mueller
August, 1980

The following papers were presented at various professional meetings and/or published:

"Concept for Reference Frames in Geodesy and Geodynamics"
AGU Spring Meeting, Miami Beach, Florida, April 17-21, 1978
IAU Symposium No. 82, Cadiz, Spain, May 8-12, 1978
7th Symposium on Mathematical Geodesy, Assisi, Italy, June 8-10, 1978
"Concepts for Reference Frames in Geodesy and Geodynamics: The Reference Directions," Bulletin Geodesique, 53 (1979), No. 3, pp. 195-213.

"What Have We Learned from Satellite Geodesy?
2nd International Symposium on Use of Artificial Satellites for Geodesy and Geodynamics, Lagonissi, Greece, May 30 - June 3, 1978

"Parameter Estimation from VLBI and Laser Ranging"
IAG Special Study Group 4.45 Meeting on Structure of the Gravity Field
Lagonissi, Greece, June 5-6, 1978

"Estimable Parameters from Spaceborne Laser Ranging"
SGRS Workshop, Austin, Texas, July 18-23, 1978

"Defining the Celestial Pole," manuscripta geodaetica, 4 (1979), No. 2 pp. 149-183.

"Three-Dimensional Geodetic Techniques"
Technology Exchange Week, Inter-American Geodetic Survey
Fort Clayton, Canal Zone, May 14-19, 1979
published in Spanish as "Tecnicas Geodesicas Tridimensionales," Memoria de la Semana de Intercambio Tecnologico, Panama, Rep. de Panama, pp. 400-426.

"On the VLBI-Satellite Laser Ranging 'Iron Triangle' Intercomparison Experiment," Meeting on Radio Interferometry Techniques for Geodesy, Massachusetts Institute of Technology, Cambridge, June 19-21, 1979

"Space Geodesy for Geodynamics, A Research Plan for the Next Decade"
Sonderforschungsbereich - Satellitengeodäsie - SFB 78
Colloquium in Viechtach, FRG, October 23-24, 1979

"Concept of Reference Frames for Geodesy and Geophysics"
seminar given at University of Stuttgart, West Germany, June 19, 1980

"Space Geodesy and Geodynamics,"
seminar given at University of Stuttgart, West Germany, June 26, 1980

"Geodetic Applications of the Global Positioning System of Satellites and Radio Interferometry," seminar given at University of Stuttgart, West Germany, July 3, 1980

"Reference Coordinate Systems for Earth Dynamics: A Preview,"
Proc. of IAU Colloquium 56 on Reference Coordinate Systems for Earth Dynamics," September 8-12, 1980, Warsaw, Poland, E.M. Gaposchkin and B. Kołaczek, eds., D. Reidel. Present at AGU, San Francisco, December, 1980.

"Comments on Conventional Terrestrial and Quasi-inertial Reference Systems," with J. Kovalevsky, Proc. of IAU Colloquium 56 on Reference Coordinate Systems for Earth Dynamics, September 8-12, 1980, Warsaw, Poland, E.M. Gaposchkin and B. Kołaczek, eds., D. Reidel.

"Precise Positioning with GPS"
seminar given at Deutsche Geodätische Forschungsinstitut, Munich, West Germany, September 18, 1980